

Robust contrastive learning and nonlinear ICA in the presence of outliers

Hiroaki Sasaki

Department of Complex and Intelligent Systems
Future University Hakodate, Japan

Takashi Takenouchi

Department of Complex and Intelligent Systems
Future University Hakodate, Japan
RIKEN AIP, Japan

Ricardo Monti

Gatsby Computational Neuroscience Unit
University College London, UK

Aapo Hyvärinen

Université Paris-Saclay Inria, CEA, France
Department of Computer Science
Helsinki Institute for Information Technology HIIT
University of Helsinki, Finland

Abstract

Nonlinear independent component analysis (ICA) is a general framework for unsupervised representation learning, and aimed at recovering the latent variables in data. Recent practical methods perform nonlinear ICA by solving a series of classification problems based on logistic regression. However, it is well-known that logistic regression is vulnerable to outliers, and thus the performance can be strongly weakened by outliers. In this paper, we first theoretically analyze nonlinear ICA models in the presence of outliers. Our analysis implies that estimation in nonlinear ICA can be seriously hampered when outliers exist on the tails of the (noncontaminated) target density, which happens in a typical case of contamination by outliers. We develop two robust nonlinear ICA methods based on the γ -divergence, which is a robust alternative to the KL-divergence in logistic regression. The proposed methods are shown to have desired robustness properties in the context of nonlinear ICA. We also experimentally demonstrate that the proposed methods are very robust and outperform existing methods in the presence of outliers. Finally, the proposed method is applied to ICA-based causal discovery and shown to find a plausible causal relationship on fMRI data.

1 Introduction

Nonlinear independent component analysis (ICA) is a principled framework for unsupervised representation learning which has generated a large amount of recent interest in learning deep neural networks. Unlike most unsupervised methods, nonlinear ICA is based on a clear statistical estimation task. The problem is rigorously formulated by defining a generative model for the data, and the goal is to recover (or identify) the mutually independent latent source components

of which the data is observed as a general nonlinear mixing. Nonlinear ICA includes a number of potential applications such as causal analysis [Monti et al., 2019] and transfer learning [Noroozi and Favaro, 2016].

In contrast to the great success of *linear* ICA [Hyvärinen and Oja, 2000], nonlinear ICA has not received so much attention until recently because the problem is fundamentally ill-posed: There are an infinite number of decompositions of a random vector into mutually independent variables [Hyvärinen and Pajunen, 1999, Locatello et al., 2019], while the identifiability proof is established in linear ICA [Comon, 1994]. Thus, in general, we cannot recover the original source components under the same conditions as linear ICA.

Novel identifiability proofs for nonlinear ICA have been recently established [Sprekeler et al., 2014, Hyvärinen and Morioka, 2016, 2017, Hyvärinen et al., 2019]. The main idea is to introduce some auxiliary variables given which the latent source components are conditionally independent. For instance, *time contrastive learning* divides time series data into a number of time segments and uses the time segment label as the auxiliary variable [Hyvärinen and Morioka, 2016]; in *permutation contrastive learning*, the auxiliary variable is the history of time-series data [Hyvärinen and Morioka, 2017]. These methods perform nonlinear ICA by solving a series of classification problems in a similar spirit as generative adversarial network [Goodfellow et al., 2014] and noise contrastive estimation [Gutmann and Hyvärinen, 2012]. Interestingly, a heuristic yet successful approach called *self-supervised learning* [Larsson et al., 2017, Noroozi and Favaro, 2016, Oord et al., 2018] also takes the same approach of solving unsupervised learning problems through classification. Thus, the theory of nonlinear ICA might shed light on the principles underlying self-supervised learning.

In order to solve the nonlinear ICA problems in practice, logistic regression has been employed [Hyvärinen and Morioka, 2016, 2017, Hyvärinen et al., 2019], which is based on (conditional) maximum likelihood estimation (MLE). MLE has a number of useful properties, but it is well-known to be vulnerable to outliers. Thus, the performance of the existing nonlinear ICA methods might be strongly degraded by outliers. This is a very important problem because outliers are ubiquitous on real-world datasets. For instance, outliers are often observed in functional MRI data to which ICA methods have been applied [Monti et al., 2019].

In this paper, we first define a contaminated density model of sources as a mixture of the (noncontaminated) target and outlier densities, and then theoretically analyze how outliers hamper estimation in nonlinear ICA. Our analysis implies that estimation in nonlinear ICA may be degraded particularly when the ratio of the outlier density to the target density can take a very large value. This large ratio happens when the outlier density lies on the tails of the target density as in a common outlier situation.

Next, we propose two robust methods for nonlinear ICA. Our methods also solve classification problems, but are based on the γ -divergence [Fujisawa and Eguchi, 2008]. γ -divergence is a generalization of KL-divergence and has a favorable robust property [Fujisawa and Eguchi, 2008, Hung et al., 2018, Kawashima and Fujisawa, 2018], which is expressed as the *super robustness* [Cichocki and Amari, 2010, Amari, 2016]: The latent bias caused from outliers can be sufficiently small even in the case of heavy contamination almost as if outliers did not exist. This is in stark contrast with the density power divergence [Basu et al., 1998], which is often theoretically proved to be robust under small contamination of outliers. We show that the γ -divergence has a desirable robust property in the context of nonlinear ICA as well, and experimentally confirm that the proposed nonlinear ICA methods are much more robust against outliers than existing methods. Finally, our robust nonlinear ICA method is applied to causal analysis and demonstrated to find a plausible causal relationship on fMRI data.

2 Background

ICA is a rigorous framework for unsupervised learning, and assumes that the d_x -dimensional vectors of observed data $\mathbf{x}(t) := (x_1(t), \dots, x_{d_x}(t))^\top$, $t = 1, \dots, T$ are generated from a nonlinear mixing of the source vectors $\mathbf{s}(t) = (s_1(t), \dots, s_{d_x}(t))^\top$ as

$$\mathbf{x}(t) = \mathbf{f}(\mathbf{s}(t)), \quad (1)$$

where $\mathbf{f}(\mathbf{s}) = (f_1(\mathbf{s}), \dots, f_{d_x}(\mathbf{s}))^\top$, and f_i denotes a smooth and invertible nonlinear function. The goal is to recover (or identify) the sources from data only.

Nonlinear ICA has been hampered by the fact that the problem is seriously ill-posed and the original sources cannot be recovered (i.e., not identifiable) under the same independence assumption as linear ICA, although there were heuristic works previously [Wiskott and Sejnowski, 2002, Harmeling et al., 2003]. Recently, novel identifiability proofs have been established together with practical algorithms [Sprekeler et al., 2014, Hyvärinen and Morioka, 2016, 2017, Hyvärinen et al., 2019]. Time contrastive learning (TCL) divides time series data $\{\mathbf{x}(t)\}_{t=1}^T$ into K time segments, and then a time segment label $u(t) = k$, $k = 1, \dots, K$ is assigned to $\mathbf{x}(t)$ in the k -th segment. A nonlinear feature $\mathbf{h}(\mathbf{x}(t)) = (h_1(\mathbf{x}(t)), \dots, h_{d_x}(\mathbf{x}(t)))^\top$ modelled by a neural network is learned via multinomial logistic regression to the *artificial* supervised dataset $\{(u(t), \mathbf{x}(t))\}_{t=1}^T$. For the identifiability, when the conditional density of \mathbf{s} given a time segment label u is conditionally independent and belongs to an exponential family as,

$$\log p^*(\mathbf{s}|u) = \sum_{j=1}^d \lambda_{u,j} q_j^*(s_j) + \lambda_{u,0} - \log Z(\boldsymbol{\lambda}_u), \quad (2)$$

where q_j^* is a scalar function, $\lambda_{u,j}$ denotes a parameter depending on u , $\boldsymbol{\lambda}_u := (\lambda_{y,0}, \lambda_{u,1}, \dots, \lambda_{u,d_x})^\top$, and $Z(\boldsymbol{\lambda}_y)$ is the partition function, then Theorem 1 in Hyvärinen and Morioka [2016] states that the learned $\mathbf{h}(\mathbf{x})$ asymptotically equals to $\mathbf{q}(\mathbf{s}) = (q_1(s_1), \dots, q_{d_x}(s_{d_x}))^\top$ up to a linear transformation.

A more general theory without the exponential family assumption (2) was established in Hyvärinen et al. [2019]. Suppose that some auxiliary data $\mathbf{u}(t)$ is available in addition to $\mathbf{x}(t)$. For instance, the time segment label in TCL can be interpreted as auxiliary data, and permutation contrastive learning employs the past information of $\mathbf{x}(t)$ (e.g, $\mathbf{u}(t) = \mathbf{x}(t-1)$) [Hyvärinen and Morioka, 2017]. In order to learn a nonlinear feature $\mathbf{h}(\mathbf{x})$, the following binary classification problem is solved by logistic regression:

$$\mathcal{D} := \{(\mathbf{x}(t), \mathbf{u}(t))\}_{t=1}^T \text{ vs. } \mathcal{D}_p := \{(\mathbf{x}(t), \mathbf{u}_p(t))\}_{t=1}^T, \quad (3)$$

where $\mathbf{u}_p(t)$ is a random permutation of $\mathbf{u}(t)$ with respect to t . Eq.(3) indicates that \mathcal{D} is drawn from the joint density of $\mathbf{x}(t)$ and $\mathbf{u}(t)$, while the underlying density of \mathcal{D}_p can be regarded as the product of marginal densities of $\mathbf{x}(t)$ and $\mathbf{u}(t)$. Under the conditional independence assumption even more general than the exponential family (2),

$$\log p^*(\mathbf{s}|\mathbf{u}) = \sum_{i=1}^{d_x} q^*(s_i|\mathbf{u}) - \log Z(\mathbf{u}), \quad (4)$$

where $Z(\mathbf{u})$ denotes the partition function and q^* is a twice differential function, it was proved that the learned \mathbf{h} equals to \mathbf{s} up to an invertible function when $p^*(\mathbf{s}|\mathbf{u})$ is sufficiently diverse and complex [Hyvärinen et al., 2019, Theorem 1].¹ However, the identifiability theory for the general case does not hold in the exponential family case (2) because the exponential family is too “simple” [Hyvärinen et al., 2019, Theorem 2]. Thus, both theories for the general and exponential cases complement each other.

The nonlinear ICA methods above employ logistic regression to learn $\mathbf{h}(\mathbf{x})$, which is based on (conditional) maximum likelihood estimation (MLE). MLE has a number of useful properties such as asymptotic efficiency [Wasserman, 2006]; on the other hand, it is well-known that MLE can be vulnerable against outliers. Thus, these nonlinear ICA methods might be sensitive to outliers. Next, we first theoretically investigate how outliers hamper estimation in nonlinear ICA, and then propose robust practical methods.

3 Influence of outliers in nonlinear ICA

This section theoretically investigates the influence of outliers in nonlinear ICA.

¹The complexity and diversity of $p^*(\mathbf{s}|\mathbf{u})$ is expressed by the *Assumption of Variability* in Hyvärinen et al. [2019].

3.1 Contaminated density model by outliers

Here, we first assume the following contaminated conditional density model of s given auxiliary variables \mathbf{u} :

$$p(\mathbf{s}|\mathbf{u}) = (1 - \epsilon(\mathbf{u}))p^*(\mathbf{s}|\mathbf{u}) + \epsilon(\mathbf{u})\delta(\mathbf{s}|\mathbf{u}), \quad (5)$$

where $\epsilon(\mathbf{u})$ is a contamination ratio in $[0, 1)$. Eq.(5) means that the sources from $p^*(\mathbf{s}|\mathbf{u})$ are *contaminated* by outliers generated from the outlier density $\delta(\mathbf{s}|\mathbf{u})$. We call $p^*(\mathbf{s}|\mathbf{u})$ the *target* density in this paper because it generates the target sources which we want to recover from data \mathbf{x} . Since $\epsilon(\mathbf{u})$ can be dependent on \mathbf{u} , the contaminated density model (5) is very general and called *heterogeneous* contamination. As theoretically shown later, our methods can accommodate heterogeneous contamination.

3.2 Influence of outliers in conditionally exponential case

As in Hyvärinen et al. [2019, Section 4.3], we first focus on the following conditionally independent and exponential family, which generalizes the exponential family (2) in TCL:

$$\log p^*(\mathbf{s}|\mathbf{u}) = \sum_{j=1}^{d_x} \lambda_j(\mathbf{u})q_j(s_j) + \lambda_0(\mathbf{u}) - \log Z(\boldsymbol{\lambda}(\mathbf{u})), \quad (6)$$

where $\boldsymbol{\lambda}(\mathbf{u}) := (\lambda_0(\mathbf{u}), \lambda_1(\mathbf{u}), \dots, \lambda_{d_x}(\mathbf{u}))^\top$. Then, we investigate how the outlier density $\delta(\mathbf{s}|\mathbf{u})$ hampers estimation in ICA, and we establish the following theorem:

Theorem 1. *First, the following assumptions are made:*

(A1) *Data \mathbf{x} is generated from (1) where \mathbf{f} is invertible.*

(A2) *$p^*(\mathbf{s}|\mathbf{u})$ is conditionally independent and belongs to the exponential family (6).*

(A3) *For all \mathbf{s} and \mathbf{u} , $\frac{\delta(\mathbf{s}|\mathbf{u})}{p^*(\mathbf{s}|\mathbf{u})}$ is finite.*

(A4) *In the limit of infinite data, $p(\mathbf{x}|\mathbf{u})$ is universally approximated as*

$$\log \frac{p(\mathbf{x}|\mathbf{u})}{c(\mathbf{x})e(\mathbf{u})} = \mathbf{w}(\mathbf{u})^\top \mathbf{h}(\mathbf{x}), \quad (7)$$

where $\mathbf{w}(\mathbf{u}) := (w_1(\mathbf{u}), \dots, w_{d_x}(\mathbf{u}))^\top$ is a vector-valued function, and c and e some scalar functions.

(A5) *There exist $m + 1$ points $\mathbf{u}_0, \mathbf{u}_1, \dots, \mathbf{u}_m$ such that the following d_x by d_x matrices are invertible: $\bar{\mathbf{\Lambda}} := \sum_{i=1}^m \bar{\boldsymbol{\lambda}}(\mathbf{u}_i)\bar{\boldsymbol{\lambda}}(\mathbf{u}_i)^\top$ and $\sum_{i=1}^m \bar{\mathbf{w}}(\mathbf{u}_i)\bar{\boldsymbol{\lambda}}(\mathbf{u}_i)^\top$, where $\bar{\boldsymbol{\lambda}}(\mathbf{u}) := \boldsymbol{\lambda}(\mathbf{u}) - \boldsymbol{\lambda}(\mathbf{u}_0)$ and $\bar{\mathbf{w}}(\mathbf{u}) := \mathbf{w}(\mathbf{u}) - \mathbf{w}(\mathbf{u}_0)$.*

Then, regarding sufficiently small $\epsilon(\mathbf{u})$ for all \mathbf{u} , in the limit of infinite data,

$$\mathbf{q}(\mathbf{s}) + \mathbf{r}(\mathbf{s}) = \mathbf{A}\mathbf{h}(\mathbf{x}) + \boldsymbol{\alpha}, \quad (8)$$

where \mathbf{A} is a d_x by d_x invertible matrix, $\boldsymbol{\alpha}$ is a d_x -dimensional vector, and with $\bar{\boldsymbol{\omega}}(\mathbf{u}) := \bar{\mathbf{\Lambda}}^{-1}\bar{\boldsymbol{\lambda}}(\mathbf{u})\mathbf{1}_{d_x} = (1, 1, \dots, 1)^\top$ and $\epsilon_{\max} := \max_{i=0,1,\dots,m} \epsilon(\mathbf{u}_i)$,

$$\mathbf{r}(\mathbf{s}) := \sum_{i=1}^m \left\{ \epsilon(\mathbf{u}_i) \frac{\delta(\mathbf{s}|\mathbf{u}_i)}{p^*(\mathbf{s}|\mathbf{u}_i)} - \epsilon(\mathbf{u}_0) \frac{\delta(\mathbf{s}|\mathbf{u}_0)}{p^*(\mathbf{s}|\mathbf{u}_0)} \right\} \bar{\boldsymbol{\omega}}(\mathbf{u}_i) + O(\epsilon_{\max}^2)\mathbf{1}_{d_x}. \quad (9)$$

The proof is deferred to Appendix A. First of all, in the case of no outliers, (8) is essentially the same identifiability result as Theorem 3 in Hyvärinen et al. [2019] as well as Theorem 1 in Hyvärinen and Morioka [2016] for TCL: $\epsilon(\mathbf{u}) = 0$ leads to $\mathbf{r}(\mathbf{s}) = \mathbf{0}$, and therefore $\mathbf{h}(\mathbf{x})$ equals to $\mathbf{q}(\mathbf{s})$ up to a linear transformation. This linear indeterminacy could be removed by some linear ICA method in postprocessing.

Again, in no outlier case (i.e., $p(\mathbf{x}|\mathbf{u}) = p^*(\mathbf{x}|\mathbf{u})$), Assumption (A4) can be written as

$$\log \frac{p^*(\mathbf{x}|\mathbf{u})}{c(\mathbf{x})e(\mathbf{u})} = \mathbf{w}(\mathbf{u})^\top \mathbf{h}(\mathbf{x}). \quad (10)$$

To satisfy (10), Hyvärinen et al. [2019] performs binary logistic regression where the log-odds ratio, $\log \frac{p^*(\mathbf{x}, \mathbf{u})}{p^*(\mathbf{x})p(\mathbf{u})}$, is approximated by $\mathbf{w}(\mathbf{u})^\top \mathbf{h}(\mathbf{x})$ where $p^*(\mathbf{x}) = \int p^*(\mathbf{x}, \mathbf{u}) d\mathbf{u}$. Eq.(10) (or Assumption (A4)) is a more general expression than the odds ratio: We do not necessarily need to accurately estimate the noncontaminated log-odds ratio, and it is sufficient to perform nonlinear ICA that the numerator is the conditional density $p^*(\mathbf{s}|\mathbf{u})$ or joint density $p^*(\mathbf{s}, \mathbf{u})$ up to the product of nonzero scalar functions of \mathbf{s} and \mathbf{u} . In fact, this is the key point for our robust method proposed in Section 4.1.

On the other hand, when $\epsilon(\mathbf{u}) \neq 0$, Theorem 1 indicates that estimation for the exponential family might be hampered by $\mathbf{r}(\mathbf{s})$. In particular, the elements in $\mathbf{r}(\mathbf{s})$ can be significantly nonzeros if the density ratio $\frac{\delta(\mathbf{s}|\mathbf{u})}{p^*(\mathbf{s}|\mathbf{u})}$ in (9) is very large. The large ratio tends to happen when $\delta(\mathbf{s}|\mathbf{u})$ lies on the tails of $p^*(\mathbf{s}|\mathbf{u})$ (i.e., very small $p^*(\mathbf{s}|\mathbf{u})$, but large $\delta(\mathbf{s}|\mathbf{u})$). Thus, since logistic regression accurately estimates the log-odds ratio of the contaminated density, existing nonlinear ICA methods might be sensitive to outliers. Therefore, it would be desirable to develop a robust nonlinear ICA method.

3.3 Influence of outliers in non-exponential case

We performed a similar contamination analysis as Theorem 1 under the general (non-exponential) conditional independence condition (4) as well, but put the details in Appendix B. The conclusion is slightly complicated yet fundamentally similar as Theorem (1): Estimation in nonlinear ICA can be hampered when the four ratios, $\frac{\delta^m(\mathbf{s}|\mathbf{u})}{p^*(\mathbf{s}|\mathbf{u})}$, $\frac{\delta^l(\mathbf{s}|\mathbf{u})}{p^*(\mathbf{s}|\mathbf{u})}$, $\frac{\delta(\mathbf{s}|\mathbf{u})}{p^*(\mathbf{s}|\mathbf{u})}$ and $\frac{\delta^{l,m}(\mathbf{s}|\mathbf{u})}{p^*(\mathbf{s}|\mathbf{u})}$, are very large where $\delta^l(\mathbf{s}|\mathbf{u}) := \frac{\partial \delta(\mathbf{s}|\mathbf{u})}{\partial s_l}$ and $\delta^{l,m}(\mathbf{s}|\mathbf{u}) := \frac{\partial^2 \delta(\mathbf{s}|\mathbf{u})}{\partial s_l \partial s_m}$ for $l, m = 1, \dots, d_x$. These ratios might be large when smooth $\delta(\mathbf{s}|\mathbf{u})$ exists on the tails of $p^*(\mathbf{s}|\mathbf{u})$. Therefore, again, it would be useful to develop a robust method in the general non-exponential case as well.

4 Robust contrastive learning

Our goal is to robustify nonlinear ICA methods. In light of the results above, the key is to estimate $\frac{p^*(\mathbf{x}|\mathbf{u})}{c(\mathbf{x})e(\mathbf{u})}$ in (10) in spite of the contamination, which holds in the non-exponential family case as well (See Appendix B for more details). To this end, this section proposes two robust methods for nonlinear ICA based on the γ -cross entropy [Fujisawa and Eguchi, 2008], and shows that the desired estimation would be possible even under contamination by outliers.

Before going to the details, let us clarify the notations: $p(\mathbf{x}|\mathbf{u})$ denotes the contaminated conditional density of \mathbf{x} given \mathbf{u} from (5), while $p^*(\mathbf{x}|\mathbf{u})$ and $\delta(\mathbf{x}|\mathbf{u})$ are the (noncontaminated) target and outlier conditional densities, respectively. We can obtain the two marginal densities from $p(\mathbf{x}|\mathbf{u})$ and $p^*(\mathbf{x}|\mathbf{u})$ as $p(\mathbf{x}) := \int p(\mathbf{x}|\mathbf{u})p(\mathbf{u})d\mathbf{u}$ and $p^*(\mathbf{x}) := \int p^*(\mathbf{x}|\mathbf{u})p(\mathbf{u})d\mathbf{u}$. In the remaining part of this paper, we may suppose that $p(\mathbf{u})$ is contaminated by an outlier density in general but the contaminated model is not explicitly defined because a specific form is not required in the analysis of this paper.

4.1 Nonlinear ICA with robust binary classification

The first method performs nonlinear ICA by solving a binary classification problem under the γ -cross entropy [Fujisawa and Eguchi, 2008, Hung et al., 2018]. Let us express a class label by y , and $y = 1$ and $y = 0$ correspond to datasets \mathcal{D} and \mathcal{D}_p in (3) which are drawn from $p(\mathbf{x}, \mathbf{u}|y = 1) = p(\mathbf{x}, \mathbf{u})$ and $p(\mathbf{x}, \mathbf{u}|y = 0) = p(\mathbf{x})p(\mathbf{u})$, respectively. Moreover,

symmetric class probabilities are assumed (i.e., $p(y = 0) = p(y = 1) = \frac{1}{2}$). Then, the γ -cross entropy for binary classification is defined as

$$d_\gamma(p(y|\mathbf{x}, \mathbf{u}), r(\mathbf{x}, \mathbf{u}); p(\mathbf{x}, \mathbf{u})) := -\frac{1}{\gamma} \log \iint \sum_{y=0}^1 \left\{ \frac{r(\mathbf{x}, \mathbf{u})^{y(\gamma+1)}}{1 + r(\mathbf{x}, \mathbf{u})^{\gamma+1}} \right\}^{\frac{\gamma}{\gamma+1}} p(y, \mathbf{x}, \mathbf{u}) d\mathbf{x} d\mathbf{u}, \quad (11)$$

where $r(\mathbf{x}, \mathbf{u})$ denotes a model (e.g., a neural network) and positive function. As proven in Fujisawa and Eguchi [2008], the γ -cross entropy has a number of remarkable properties. For instance, $d_\gamma(p(y|\mathbf{x}, \mathbf{u}), r(\mathbf{x}, \mathbf{u}); p(\mathbf{x}, \mathbf{u}))$ approaches to the cross entropy in logistic regression as $\gamma \rightarrow 0$. Notably, the γ -cross entropy has a desired robustness property on parameter estimation even in the heavy contamination of outliers [Fujisawa and Eguchi, 2008, Kanamori and Fujisawa, 2015, Kawashima and Fujisawa, 2018]. Next, we show that the robust property holds in the context of nonlinear ICA.

Robustness to heavy contamination of outliers in nonlinear ICA: First, we establish the following theorem to understand under what conditions a good estimation in the presence of outliers is possible for nonlinear ICA:

Theorem 2. *Assume that*

$$\nu := \iint \left\{ \frac{r(\mathbf{x}, \mathbf{u})^{\gamma+1}}{1 + r(\mathbf{x}, \mathbf{u})^{\gamma+1}} \right\}^{\frac{\gamma}{\gamma+1}} \epsilon(\mathbf{u}) \delta(\mathbf{x}, \mathbf{u}) d\mathbf{x} d\mathbf{u} \quad (12)$$

is sufficiently small. Then, it holds that

$$d_\gamma(p(y|\mathbf{x}, \mathbf{u}), r(\mathbf{x}, \mathbf{u}); p(\mathbf{x}, \mathbf{u})) = J[r(\mathbf{x}, \mathbf{u}); (1 - \epsilon(\mathbf{u}))p^*(\mathbf{x}, \mathbf{u}), p(\mathbf{x})p(\mathbf{u})] + O(\nu), \quad (13)$$

where

$$J[r(\mathbf{x}, \mathbf{u}); (1 - \epsilon(\mathbf{u}))p^*(\mathbf{x}, \mathbf{u}), p(\mathbf{x})p(\mathbf{u})] := -\frac{1}{\gamma} \log \left[\frac{1}{2} \iint \left\{ \frac{1}{1 + r(\mathbf{x}, \mathbf{u})^{\gamma+1}} \right\}^{\frac{\gamma}{\gamma+1}} p(\mathbf{x})p(\mathbf{u}) d\mathbf{x} d\mathbf{u} + \frac{1}{2} \iint \left\{ \frac{r(\mathbf{x}, \mathbf{u})^{\gamma+1}}{1 + r(\mathbf{x}, \mathbf{u})^{\gamma+1}} \right\}^{\frac{\gamma}{\gamma+1}} (1 - \epsilon(\mathbf{u}))p^*(\mathbf{x}, \mathbf{u}) d\mathbf{x} d\mathbf{u} \right].$$

Furthermore, under the assumption that $p(\mathbf{x})$, $p(\mathbf{u})$ and $r(\mathbf{x}, \mathbf{u})$ are positive for all \mathbf{x} and \mathbf{u} , $J[r(\mathbf{x}, \mathbf{u}); (1 - \epsilon(\mathbf{u}))p^*(\mathbf{x}, \mathbf{u}), p(\mathbf{x})p(\mathbf{u})]$ is minimized at

$$r^*(\mathbf{x}, \mathbf{u}) = \frac{(1 - \epsilon(\mathbf{u}))p^*(\mathbf{x}|\mathbf{u})}{p(\mathbf{x})}. \quad (14)$$

The proof is deferred to Appendix C. Theorem 2 indicates that under the condition that ν is sufficiently small, we could obtain a desirable estimation result (14) in nonlinear ICA: Eq.(14) is the special case of the ideal universal approximation condition (10) without outliers where $c(\mathbf{x}) = p(\mathbf{x})$ and $e(\mathbf{u}) = 1/(1 - \epsilon(\mathbf{u}))$. The notable point is that $\epsilon(\mathbf{u})$ is never assumed to be small in itself. Thus, heavy contamination of outliers is also within the scope of our method.

Let us define the supports of $p^*(\mathbf{s}|\mathbf{u})$ and $\delta(\mathbf{s}|\mathbf{u})$ as

$$\mathcal{S}_u^{p^*} := \{\mathbf{s} \mid p^*(\mathbf{s}|\mathbf{u}) > 0\}, \quad \mathcal{S}_u^\delta := \{\mathbf{s} \mid \delta(\mathbf{s}|\mathbf{u}) > 0\},$$

respectively. Then, the following proposition gives insight into when ν is sufficiently small:

Proposition 1. *Let us denote the domains of \mathbf{u} and \mathbf{s} by \mathcal{U} and \mathcal{S} , respectively. We assume that (i) the integrals in ν are defined over \mathcal{U} and \mathcal{S} , (ii) data \mathbf{x} is generated from (1) with an invertible nonlinear mixing function \mathbf{f} , (iii) $\mathcal{S}_u^{p^*} \cap \mathcal{S}_u^\delta = \emptyset$, and (iv) $p(\mathbf{s}) \neq 0$ on \mathcal{S} . For $\gamma > 0$,*

$$\nu \leq O \left(\sup_{\mathbf{x}, \mathbf{u}} |r(\mathbf{x}, \mathbf{u}) - r^*(\mathbf{x}, \mathbf{u})| \right).$$

The proof is given in Appendix D. The most important condition is $\mathcal{S}_u^{p^*} \cap \mathcal{S}_u^\delta = \emptyset$, which implies that $p^*(s|\mathbf{u})$ and $\delta(s|\mathbf{u})$ are *separated* on \mathcal{S} . For instance, $p^*(s|\mathbf{u})$ and $\delta(s|\mathbf{u})$ are the uniform densities on $[0, 1]^{d_x}$ and $[2, 3]^{d_x}$ respectively, their supports are nonoverlapping and thus separated. Therefore, Proposition 1 implies that ν can be sufficiently small in the neighborhood of $r^*(\mathbf{x}, \mathbf{u})$ when $\delta(s|\mathbf{u})$ and $p^*(s|\mathbf{u})$ are clearly *separated*. This density separation would happen approximately on a situation where $\delta(s|\mathbf{u})$ exists on the tails of $p^*(s|\mathbf{u})$ as in a common outlier situation.

On the other hand, when $\gamma = 0$ (i.e., logistic regression), it can be easily confirmed from the definition (12) that ν is a nonzero constant and cannot be sufficiently small. Thus, nonlinear ICA methods based on logistic regression can be more sensitive to outliers. Appendix E includes another discussion that the γ -entropy evades the influence of the large density ratio $\delta(s|\mathbf{u})/p^*(s|\mathbf{u})$, which is one of the main factors to hamper estimation in nonlinear ICA as already indicated in Section 3, while the logistic regression might not be able to avoid the strong influence from $\delta(s|\mathbf{u})/p^*(s|\mathbf{u})$.

Influence function analysis: Next, we investigate the robustness of our nonlinear ICA method based on the influence function (IF), which is an established measure in robust statistics [Hampel et al., 2011]. To this end, let us define the following contaminated density model:

$$\begin{aligned}\bar{p}(\mathbf{x}, \mathbf{u}) &= (1 - \epsilon)p^*(\mathbf{x}, \mathbf{u}) + \epsilon\bar{\delta}_{(\bar{\mathbf{x}}, \bar{\mathbf{u}})}(\mathbf{x}, \mathbf{u}) \\ \bar{p}(\mathbf{x}) &= (1 - \epsilon)p^*(\mathbf{x}) + \epsilon\bar{\delta}_{\bar{\mathbf{x}}}(\mathbf{x}) \\ \bar{p}(\mathbf{u}) &= (1 - \epsilon)p^*(\mathbf{u}) + \epsilon\bar{\delta}_{\bar{\mathbf{u}}}(\mathbf{u}),\end{aligned}$$

where $\epsilon \in [0, 1)$ is a contamination ratio, $\bar{\delta}_z$ is the Dirac delta function having a point mass at z . We suppose that a model $r_\theta(\mathbf{x}, \mathbf{u})$ is positive and parameterized by θ , and define $\hat{\theta}$ as a solution of the estimating function $\frac{\partial}{\partial \theta} d_\gamma(p^*(y|\mathbf{x}, \mathbf{u}), r_\theta(\mathbf{x}, \mathbf{u}); p^*(\mathbf{x}, \mathbf{u})) = \mathbf{0}$ over the (uncontaminated) target densities where $p^*(\mathbf{x}, \mathbf{u}|y = 1) = p^*(\mathbf{x}, \mathbf{u})$ and $p^*(\mathbf{x}, \mathbf{u}|y = 0) = p^*(\mathbf{x})p^*(\mathbf{u})$. Similarly, $\hat{\theta}_\epsilon$ is defined as a solution of $\frac{\partial}{\partial \theta} d_\gamma(\bar{p}(y|\mathbf{x}, \mathbf{u}), r_\theta(\mathbf{x}, \mathbf{u}); \bar{p}(\mathbf{x}, \mathbf{u})) = \mathbf{0}$ over the contaminated densities where $\bar{p}(\mathbf{x}, \mathbf{u}|y = 1) = \bar{p}(\mathbf{x}, \mathbf{u})$ and $\bar{p}(\mathbf{x}, \mathbf{u}|y = 0) = \bar{p}(\mathbf{x})\bar{p}(\mathbf{u})$. Then, IF is defined by

$$\text{IF}(\bar{\mathbf{x}}, \bar{\mathbf{u}}) = \lim_{\epsilon \rightarrow 0} \frac{\hat{\theta} - \hat{\theta}_\epsilon}{\epsilon}. \quad (15)$$

Eq.(15) indicates that IF measures how $\hat{\theta}$ is influenced by outliers $(\bar{\mathbf{x}}, \bar{\mathbf{u}})$ in the small contamination, and a larger IF implies that $\hat{\theta}$ is more sensitive to outliers. *B-robustness* is a desired property for $\hat{\theta}$ in terms of IF: $\hat{\theta}$ is said to be B-robust when $\sup_{\bar{\mathbf{x}}, \bar{\mathbf{u}}} |\text{IF}(\bar{\mathbf{x}}, \bar{\mathbf{u}})| < \infty$ [Hampel et al., 2011]. The following proposition shows that the solution of our method based on the γ -cross entropy can be B-robust under mild assumptions:

Proposition 2. Assume that a matrix C_θ is invertible², and $r_\theta(\mathbf{x}, \mathbf{u})$ satisfies

$$\lim_{|r_\theta(\mathbf{x}, \mathbf{u})| \rightarrow \infty} S_\theta(\mathbf{x}, \mathbf{u}) \frac{\partial \log r_\theta(\mathbf{x}, \mathbf{u})^{(\gamma+1)}}{\partial \theta} = 0, \quad (16)$$

where $S_\theta(\mathbf{x}, \mathbf{u}) := \{L_\theta(\mathbf{x}, \mathbf{u})(1 - L_\theta(\mathbf{x}, \mathbf{u}))\}^{\frac{\gamma}{1+\gamma}}$ with $L_\theta(\mathbf{x}, \mathbf{u}) := \frac{1}{1+r_\theta(\mathbf{x}, \mathbf{u})^{(\gamma+1)}}$. Then, for $\gamma > 0$,

$$\sup_{\bar{\mathbf{x}}, \bar{\mathbf{u}}} |\text{IF}(\bar{\mathbf{x}}, \bar{\mathbf{u}})| < \infty. \quad (17)$$

The proof is given in Appendix F. Proposition 2 indicates that our method can be B-robust when $r_\theta(\mathbf{x}, \mathbf{u})$ is modelled by a continuous yet unbounded function (possibly, feedforward neural networks with unbounded activation functions). Assumption (16) is mild because when $|r_\theta(\mathbf{x}, \mathbf{u})|$ diverges to infinite as $\|\mathbf{x}\|, \|\mathbf{u}\| \rightarrow \infty$ as in neural networks, $S_\theta(\mathbf{x}, \mathbf{u})$ quickly approaches 0.

On the other hand, in the limit of $\gamma = 0$ (i.e., logistic regression), a class of models for $r_\theta(\mathbf{x}, \mathbf{u})$, which satisfies Assumption (16), is very limited because $S_\theta(\mathbf{x}, \mathbf{u}) = 1$. For instance, when $r_\theta(\mathbf{x}, \mathbf{u})$ is a neural network with an unbounded activation function, Assumption (16) would not hold. Thus, our analysis implies that the γ -cross entropy is promising for nonlinear ICA in the presence of outliers.

²The definition of C_θ is left in Appendix F because it is very complicated.

Robust permutation contrastive learning (RPCL): As a practical method, we propose a robust variant of permutation contrastive learning (PCL) [Hyvärinen and Morioka, 2017] which we call *robust permutation contrastive learning* (RPCL). The original PCL supposes that sources are temporally dependent (e.g., $\mathbf{s}(t)$ and $\mathbf{s}(t-1)$ are statistically dependent), and then makes use of the temporal dependencies for nonlinear ICA by regarding past information as the auxiliary variable $\mathbf{u}(t) = \mathbf{x}(t-1)$. PCL belongs to the non-exponential family case (4).

RPCL estimates a model $r(\mathbf{x}, \mathbf{u})$ based on the following empirical γ -cross entropy for binary classification:

$$\begin{aligned} & \widehat{d}_\gamma(p(y|\mathbf{x}, \mathbf{u}), r(\mathbf{x}, \mathbf{u}); p(\mathbf{x}, \mathbf{u})) \\ & := -\frac{1}{\gamma} \log \left[\frac{1}{2T} \sum_{t=1}^n \left\{ \left(\frac{r(\mathbf{x}(t), \mathbf{u}(t))^{\gamma+1}}{1 + r(\mathbf{x}(t), \mathbf{u}(t))^{\gamma+1}} \right)^{\frac{\gamma}{\gamma+1}} + \left(\frac{1}{1 + r(\mathbf{x}(t), \mathbf{u}_p(t))^{\gamma+1}} \right)^{\frac{\gamma}{\gamma+1}} \right\} \right], \end{aligned}$$

where $\mathbf{u}_p(t)$ denotes a random permutation of $\mathbf{u}(t)$ with respect to t . Based on the universal approximation assumption in Hyvärinen and Morioka [2017, Theorem 1 and Eq.(12)] or Appendix B, we restrict a model r as $r(\mathbf{x}(t), \mathbf{u}(t)) = \exp(\sum_{i=1}^{d_x} \psi_i(h_i(\mathbf{x}(t)), h_i(\mathbf{u}(t))))$ with a neural network $\mathbf{h}(\mathbf{x}) = (h_1(\mathbf{x}), \dots, h_{d_x}(\mathbf{x}))^\top$. Following Hyvärinen and Morioka [2017], $\psi_i(h_i(\mathbf{x}), h_i(\mathbf{u}))$ was further modelled by $|a_{i,1}h_i(\mathbf{x}) + a_{i,2}h_i(\mathbf{u}) + b_i| - (\bar{a}_i h_i(\mathbf{x}) + \bar{b}_i)^2 + c$, where $a_{i,1}, a_{i,2}, b_i, \bar{a}_i, \bar{b}_i, c$ are parameters to be estimated from data. A minibatch stochastic gradient method is employed to optimize all parameters.

4.2 Nonlinear ICA with robust multiclass classification

The second method is intended for the case where the auxiliary variable $u \in \{1, \dots, K\}$ is a one-dimensional and K -discrete variable (e.g., class label). To this end, we solve a multiclass classification problem based on the γ -cross entropy:

$$d_\gamma(p(u|\mathbf{x}), r(u, \mathbf{x}); p(\mathbf{x})) := -\frac{1}{\gamma} \log \int \left\{ \frac{\sum_{u=1}^K r(u, \mathbf{x})^\gamma p(u|\mathbf{x})}{\left(\sum_{u'=1}^K r(u', \mathbf{x})^{\gamma+1} \right)^{\frac{\gamma}{\gamma+1}}} \right\} p(\mathbf{x}) d\mathbf{x}, \quad (18)$$

where we supposed $p(u=1) = p(u=2) = \dots = p(u=K)$. Regarding multiclass classification, a robustness property similar to what we had above holds by modifying the above discussion on binary classification (11) or following Kawashima and Fujisawa [2018]. When $p^*(\mathbf{s}|u)$ and $\delta(\mathbf{s}|u)$ are clearly *separated*, minimization of $d_\gamma(p(u|\mathbf{x}), r(u, \mathbf{x}); p(\mathbf{x}))$ would enable us to estimate $p^*(\mathbf{x}|u)$, which is an ideal estimation result and a special case of $\frac{p^*(\mathbf{x}|u)}{c(\mathbf{x})e(u)}$ in (10). Details are given in Appendix G.

Robust time contrastive learning (RTCL): As a practical method in multiclass classification, we propose *robust time contrastive learning* (RTCL) which is a robust version of TCL based on the γ -cross entropy (18). Both TCL and RTCL are intended for the conditional independent exponential family case (2), and suppose time series data (artificially or manually) divided into K time segments, and the auxiliary variable $u \in \{1, \dots, K\}$ is the time segment label. RTCL employs the following empirical γ -cross entropy:

$$\widehat{d}_\gamma(p(u|\mathbf{x}, \mathbf{u}), r(\mathbf{x}, \mathbf{u}); p(\mathbf{x})) := -\frac{1}{\gamma} \log \left[\frac{1}{T} \sum_{t=1}^T \left\{ \frac{\left(\sum_{k=1}^K \delta_{u(t),k} r(u(t), \mathbf{x}(t))^\gamma \right)}{\left(\sum_{u'=1}^K r(u', \mathbf{x}(t))^{\gamma+1} \right)^{\frac{\gamma}{\gamma+1}}} \right\} \right],$$

where $u(t) \in \{1, \dots, K\}$ are the observations of time-segment labels, and $\delta_{u(t),k}$ denotes the Kronecker delta. Based on the universal approximation assumption (A4) in Theorem 1, we restrict r as $r(\mathbf{x}, u) = \exp(\mathbf{w}_u^\top \mathbf{h}(\mathbf{x}) + b_u)$ for $u = 1, \dots, K$ where $\mathbf{h}(\mathbf{x})$ denotes nonlinear ICA features modelled by a neural network, and \mathbf{w}_u and b_u are parameters for weights and bias, respectively. In practice, all parameters are optimized by a minibatch stochastic gradient method.

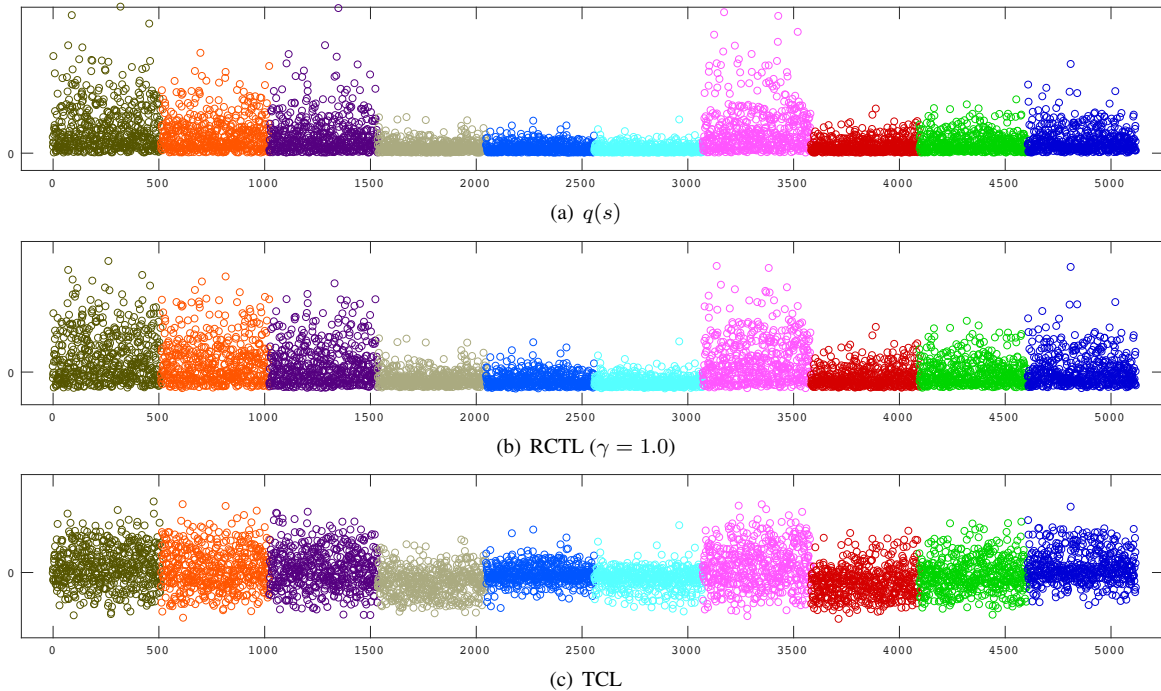


Figure 1: (a) $q(s) = |s|$ without outliers and ICA features $h(x)$ estimated by (b) RTCL and (c) TCL on ten time segments. Each time segment is highlighted by a color. The outlier density is the Laplace density, and $\epsilon = 0.1$.

5 Numerical experiments on artificial data

This section numerically investigates the robustness of RTCL and RPCL with comparison to existing nonlinear ICA methods on artificial data.

5.1 Robust time contrastive learning

Data generation, nonlinear ICA methods, evaluation: We slightly modified the experimental setting of TCL³ in Hyvärinen and Morioka [2016]. Let us note that TCL is a nonlinear ICA method specialized in the conditionally independent exponential family (2). Source vectors with time segment length 512 was first generated from (5): Following (2), given a time segment label, $p^*(s|u)$ was conditionally independent Laplace distributions with means 0 and different scales across time segments, which were randomly determined from the uniform distribution on $[0, \frac{1}{\sqrt{2}}]$. Regarding the outlier density $\delta(s|u)$, two types of densities were used: An independent Laplace distribution with mean 0 and scale 3.0, and a modulated mixture of two Gaussians where the mixing coefficients are 0.5 and the standard deviations are fixed at 0.5, but the mean parameters depend on the time segments u and were randomly determined by the uniform density on $[1.0, 4.0]$ and $[-4.0, -1.0]$, respectively. We set $\epsilon(u) = \epsilon$ for all time segments u . The total numbers of segments and of data samples were $K = 256$ and $T = 512 \times 256$ respectively, while the dimensionality of data was $d_x = 10$. Then, data x was generated according to (1) where $f(s)$ was modelled by a three-layer neural network with the leaky ReLU activation function and random weights. The numbers of all hidden and output units were the same as the dimensionality of data. As preprocessing, we performed whitening based on the γ -divergence [Chen et al., 2013].

ICA features $h(x)$ both in RTCL and TCL were modelled by a three layer neural network where the number of hidden units was $4d_x$, but the final layer was d_x . Regarding the activation functions, the final layer employed the absolute

³<https://github.com/hirosm/TCL>

Table 1: TCL and RTCL on artificial data. Averages of mean absolute correlations are computed over 10 runs. The outlier densities are the independent Laplace density and the modulated mixture of two Gaussians in the top and bottom panels, respectively. A larger value indicates a better result. The best and comparable methods judged by the t-test at the significance level 5% are described in boldface.

Laplace	TCL	RTCL ($\gamma = 0.1$)	RTCL ($\gamma = 0.3$)	RTCL ($\gamma = 0.5$)	RTCL ($\gamma = 1$)
$\epsilon = 0.01$	0.890(0.010)	0.933(0.011)	0.974(0.009)	0.985(0.010)	0.993(0.010)
$\epsilon = 0.03$	0.810(0.017)	0.865(0.013)	0.919(0.015)	0.947(0.015)	0.976(0.014)
$\epsilon = 0.05$	0.751(0.039)	0.800(0.026)	0.869(0.012)	0.898(0.017)	0.947(0.019)
$\epsilon = 0.1$	0.627(0.032)	0.690(0.058)	0.787(0.023)	0.832(0.024)	0.893(0.014)

Gaussian	TCL	RTCL ($\gamma = 0.1$)	RTCL ($\gamma = 0.3$)	RTCL ($\gamma = 0.5$)	RTCL ($\gamma = 1$)
$\epsilon = 0.01$	0.948(0.005)	0.981(0.007)	0.992(0.004)	0.995(0.002)	0.997(0.002)
$\epsilon = 0.03$	0.751(0.030)	0.876(0.033)	0.949(0.009)	0.968(0.007)	0.980(0.007)
$\epsilon = 0.05$	0.724(0.036)	0.753(0.046)	0.876(0.041)	0.924(0.022)	0.958(0.011)
$\epsilon = 0.1$	0.778(0.035)	0.757(0.035)	0.822(0.026)	0.862(0.012)	0.914(0.012)

value function, while the other hidden layers were the max-out function [Goodfellow et al., 2013] with two groups. ℓ_2 regularization was employed with the regularization parameter 10^{-4} . When $\epsilon < 0.1$, we optimized the network parameters both in RTCL and TCL with 0.001 learning rate using the Adam optimizer [Kingma and Ba, 2015] for 1,000 epochs with mini-batch size 256, while we updated the parameters for 3,000 epochs for $\epsilon = 0.1$. Regarding RTCL, to avoid bad local optima, we initialized the network parameters in RTCL by the parameters optimized by TCL for 300 epochs. As postprocessing, FastICA [Hyvärinen, 1999] was finally applied to the estimated features $\mathbf{h}(\mathbf{x})$ both in TCL and RTCL as done in Hyvärinen and Morioka [2016].

When evaluating the performances of TCL and RTCL, sources without outliers were used. Then, the performance was measured by the Pearson correlation coefficient between the absolute values of the estimated sources and of the original sources (i.e., $|\mathbf{h}(\mathbf{x})|$ after FastICA and $\mathbf{q}(s)$).

Results: Fig.1 illustrates examples of the ICA features $\mathbf{h}(\mathbf{x})$ by RTCL and TCL. Compared with the original $\mathbf{q}(s) = |s|$ (one-dimensional source) (Fig.1(a)), RTCL captures the nonstationary of the original source and well-recovers $\mathbf{q}(s)$ (Fig.1(b)). On the other hand, TCL does not recover $\mathbf{q}(s)$ at all (Fig.1(c)). This result supports the conclusion of Theorem 1 that TCL can be sensitive to outliers.

The top panel in Table 1 quantitatively indicates that RTCL is more robust against outliers than TCL. As the contamination ratio ϵ increases, the performance of TCL deteriorates. On the other hand, RTCL keeps high-correlation values even for larger γ . When the outlier density $\delta(\mathbf{x}|u)$ is the modulated mixture of two Gaussians, RTCL still performs well (bottom panel in Table 1).

5.2 Robust permutation contrastive learning

Data generation, nonlinear ICA methods, evaluation: We followed the experimental setting of PCL in Hyvärinen and Morioka [2017]. Let us note that PCL is a special case of nonlinear ICA for the non-exponential case (4). First, the temporally dependent T sources were generated from

$$\log p^*(s(t)|s(t-1)) = - \sum_{i=1}^{d_x} |s_i(t) - \rho s_i(t-1)| + C$$

where C denotes a constant and the auto-regressive coefficient ρ was fixed at 0.7. The total number of sources was $T = 65536$. Then, we randomly replaced the sources by outliers based on a constant contamination ratio ϵ , which were

Table 2: RPCL and PCL on artificial data. Averages of mean absolute correlations are computed over 10 runs.

	PCL	RPCL ($\gamma = 0.5$)	RPCL ($\gamma = 1$)	RPCL ($\gamma = 5$)	RPCL ($\gamma = 10$)
$\epsilon = 0.01$	0.917(0.028)	0.935(0.010)	0.942(0.023)	0.934(0.026)	0.911(0.027)
$\epsilon = 0.05$	0.904(0.022)	0.917(0.015)	0.926(0.008)	0.932(0.024)	0.899(0.030)
$\epsilon = 0.1$	0.854(0.053)	0.884(0.034)	0.888(0.029)	0.912(0.026)	0.886(0.023)
$\epsilon = 0.15$	0.803(0.058)	0.819(0.056)	0.838(0.048)	0.851(0.056)	0.866(0.031)

generated from the independent Laplace density with the mean 0 and scale 3. To generate \mathbf{x} , the sources with outliers are nonlinearly mixed by the same neural networks as previous experiments.

ICA features $\mathbf{h}(\mathbf{x})$ both in RPCL and PCL were modelled by the same neural networks as in the experiments for RTCL except for that no activation function was applied to the outputs on the last layer. ℓ_2 regularization was employed with the regularization parameter 10^{-4} . Then, we optimized the parameters in RPCL and PCL with 0.001 learning rate using Adam for 1,000 epochs with mini-batch size 128.⁴ Regarding RPCL, to avoid bad local optima, all parameters in RPCL are initialized by the parameters optimized by PCL for 100 epochs. Unlike the experiments in RTCL, no postprocessing was applied. The performance was measured by the Pearson correlation coefficient between learned ICA features $\mathbf{h}(\mathbf{x})$ and \mathbf{s} without outliers.

Results: Table 2 clearly shows that the correlation for PCL quickly decreases as the contaminating ratio ϵ increases. On the other hand, RPCL works significantly better than PCL even for large ϵ . Thus, our methods based on the γ -cross entropy are promising.

6 Application to causal discovery of Hippocampal fMRI data

An important application of nonlinear ICA is causal discovery whose objective is to learn the causal structure from observed data without relying on interventions [Pearl, 2000]. The use of linear ICA methods is well-established in causal discovery [Shimizu et al., 2006], and TCL has also been employed recently [Monti et al., 2019].

To demonstrate its applicability on a realworld dataset, we apply RTCL to causal discovery on resting-state fMRI data, which is well-known to contain outliers due to measurement issues such as head movement and variability in vascular health across a cohort of subjects [Poldrack et al., 2011]. The dataset we consider corresponds to resting state fMRI data collected from a single subject (caucasian male, 45 years old) over 84 successive days [Poldrack et al., 2015]. Here, each day is treated as a distinct experimental condition. Fig.2 visualizes the presence of outliers in the time series data for the Parahippocampal brain region.

We follow a TCL-based method for nonlinear causal discovery [Monti et al., 2019]. Let us consider the problem of causal discovery for bivariate data $\mathbf{x} = (x_1, x_2)^\top$. The goal of causal discovery is to determine whether x_1 causes x_2 or x_2 causes x_1 (i.e., $x_1 \rightarrow x_2$ or $x_2 \rightarrow x_1$), or to conclude that no acyclic causal relation exists. If the true causal direction is $x_1 \rightarrow x_2$, the (possibly) structural equation model (SEM) [Pearl, 2000] can be written as

$$x_1 = f_1(n_1), \quad x_2 = f_2(x_1, n_2), \quad (19)$$

where n_1 and n_2 are latent disturbances and assumed to be statistically independent each other. As discussed in Monti et al. [2019], the nonlinear SEM (19) has a clear connection to the data generative model (1) in nonlinear ICA. Roughly, the disturbance variables $(n_1, n_2)^\top$ in SEM corresponds the latent sources $(s_1, s_2)^\top$ in ICA up to their permutation. Thus, regarding the recovered sources by nonlinear ICA as estimates of $(n_1, n_2)^\top$, we could determine the causal direction by performing a series of independence tests with the observations of $\mathbf{x} = (x_1, x_2)^\top$. For instance, under the assumption that

⁴Regarding only for a few runs on the whole experiments, the learning rate in RPCL was decreased as the number of iterations increased for numerical stability

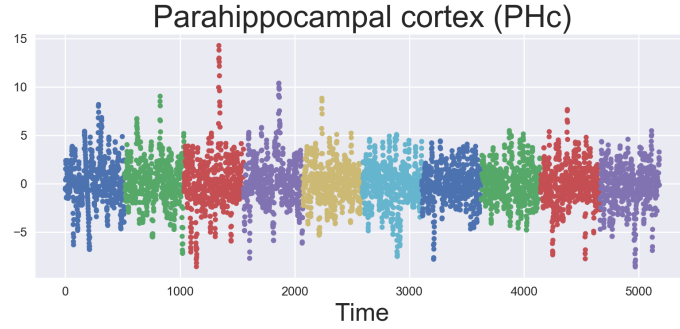


Figure 2: Subset of time series data corresponding to the Parahippocampal (PHc) region taken from the Hippocampal fMRI dataset. Different colors denote distinct segments, which in this case correspond to fMRI measurements from the same subject on distinct days.

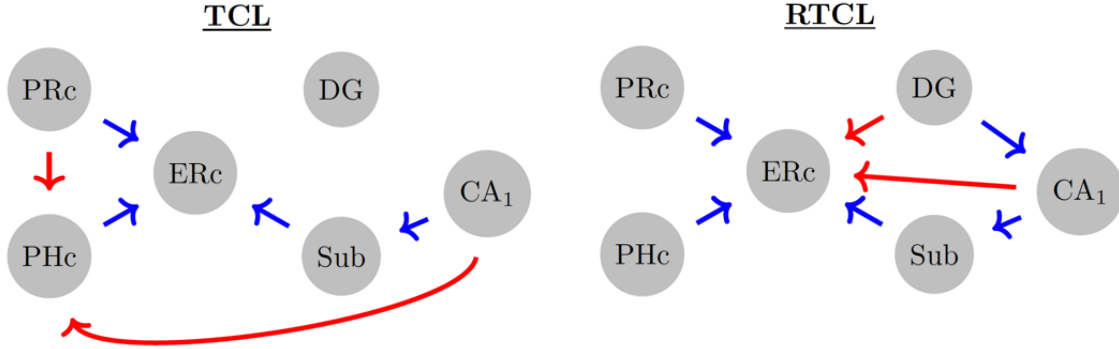


Figure 3: Estimated directed acyclic graphs based on TCL (left panel) and RTCL (right panel, $\gamma = 2.5$). For RTCL, the γ value was selected based on classification accuracy for validation data.

the true causal direction is $x_1 \rightarrow x_2$, we need to verify that $x_1 \perp\!\!\!\perp n_2$ while $x_1 \not\perp\!\!\!\perp n_1$, $x_2 \not\perp\!\!\!\perp n_1$ and $x_2 \not\perp\!\!\!\perp n_2$ [Monti et al., 2019, Property 1] by applying some independent test where $\perp\!\!\!\perp$ (or $\not\perp\!\!\!\perp$) denotes statistical independence (or dependence). Here, we employed Hilbert-Schmidt independence criteria [Gretton et al., 2005] for independence test. This approach for bivariate data is extended to multivariate data in Monti et al. [2019, Section 3.5].

Fig. 3 shows the causal structures obtained via TCL by Monti et al. [2019], and RTCL where a five layer neural network is used. Blue arrows denote edges which are plausible given the anatomical connectivity, while red arrows are not compatible with the known anatomical structure. We note that in the case of RTCL, the erroneous edges (highlighted in red) actually correspond to indirect causal effects. For example, see the edge between the Cornu Ammonis 1 (CA_1) node and the entorhinal cortex (ERc) node. While a direct connection between such nodes is anatomically implausible, there is an indirect effect which is mediated by the subiculum (Sub) node. This is in stark contrast with the results provided by TCL, where erroneous edges (highlighted in red) are not compatible with the anatomical structure (e.g., the TCL edge between CA_1 and PHc cannot be explained as an indirect causal effect).

7 Conclusion

We first analyzed the estimation of nonlinear ICA models in the presence of outliers, and then proposed two robust methods for nonlinear ICA. We showed by theoretical analysis that our methods have robustness properties in the context

of nonlinear ICA. The robustness was further empirically shown in simulations, and applicability to real-data was also demonstrated through causal discovery.

Acknowledgement

The authors would like to thank Dr. Hiroshi Morioka for sharing his PCL codes with us.

A Proof of Theorem 1

Proof. Let us express the inverse of \mathbf{f} in (5) by \mathbf{g} such that $\mathbf{s} = \mathbf{g}(\mathbf{x})$. The change of variables provides

$$\begin{aligned} \log p(\mathbf{x}|\mathbf{u}) &= \log \{ (1 - \epsilon(\mathbf{u}))p^*(\mathbf{g}(\mathbf{x})|\mathbf{u}) + \epsilon(\mathbf{u})\delta(\mathbf{g}(\mathbf{x})|\mathbf{u}) \} + \log |\det \mathbf{J}_{\mathbf{g}}(\mathbf{x})| \\ &= \log \{ p^*(\mathbf{g}(\mathbf{x})|\mathbf{u}) + \epsilon(\mathbf{u})(\delta(\mathbf{g}(\mathbf{x})|\mathbf{u}) - p^*(\mathbf{g}(\mathbf{x})|\mathbf{u})) \} + \log |\det \mathbf{J}_{\mathbf{g}}(\mathbf{x})| \\ &= \log \left[p^*(\mathbf{g}(\mathbf{x})|\mathbf{u}) \left\{ 1 + \epsilon(\mathbf{u}) \left(\frac{\delta(\mathbf{g}(\mathbf{x})|\mathbf{u})}{p^*(\mathbf{g}(\mathbf{x})|\mathbf{u})} - 1 \right) \right\} \right] + \log |\det \mathbf{J}_{\mathbf{g}}(\mathbf{x})| \\ &= \log p^*(\mathbf{g}(\mathbf{x})|\mathbf{u}) + \epsilon(\mathbf{u}) \left(\frac{\delta(\mathbf{g}(\mathbf{x})|\mathbf{u})}{p^*(\mathbf{g}(\mathbf{x})|\mathbf{u})} - 1 \right) + O(\epsilon(\mathbf{u})^2) + \log |\det \mathbf{J}_{\mathbf{g}}(\mathbf{x})|, \end{aligned}$$

where we applied $\log(1 + \epsilon(\mathbf{u})z) = \epsilon(\mathbf{u})z + O(\epsilon(\mathbf{u})^2)$ with a sufficiently small $\epsilon(\mathbf{u})$ on the last line. Then, the conditionally exponential family assumption (A2) gives

$$\log p(\mathbf{x}|\mathbf{u}) = \sum_{j=1}^d \lambda_j(\mathbf{u})q_j(g_j(\mathbf{x})) + \lambda_0(\mathbf{u}) + \epsilon(\mathbf{u}) \left(\frac{\delta(\mathbf{g}(\mathbf{x})|\mathbf{u})}{p^*(\mathbf{g}(\mathbf{x})|\mathbf{u})} - 1 \right) + O(\epsilon(\mathbf{u})^2) + \log |\det \mathbf{J}_{\mathbf{g}}(\mathbf{x})| - \log Z(\boldsymbol{\lambda}(\mathbf{u})).$$

Contrasting two log-conditional densities of \mathbf{x} given \mathbf{u} and an arbitrary fixed point \mathbf{u}_0 yields

$$\begin{aligned} \log p(\mathbf{x}|\mathbf{u}) - \log p(\mathbf{x}|\mathbf{u}_0) &= (\boldsymbol{\lambda}(\mathbf{u}) - \boldsymbol{\lambda}(\mathbf{u}_0))^\top \mathbf{q}(\mathbf{g}(\mathbf{x})) + \left\{ \epsilon(\mathbf{u}) \frac{\delta(\mathbf{g}(\mathbf{x})|\mathbf{u})}{p^*(\mathbf{g}(\mathbf{x})|\mathbf{u})} - \epsilon(\mathbf{u}_0) \frac{\delta(\mathbf{g}(\mathbf{x})|\mathbf{u}_0)}{p^*(\mathbf{g}(\mathbf{x})|\mathbf{u}_0)} \right\} \\ &\quad + O(\epsilon(\mathbf{u})^2) + O(\epsilon(\mathbf{u}_0)^2) - (\log Z(\boldsymbol{\lambda}(\mathbf{u})) - \log Z(\boldsymbol{\lambda}(\mathbf{u}_0))), \end{aligned} \quad (20)$$

where $\boldsymbol{\lambda}(\mathbf{u}) := (\lambda_0(\mathbf{u}), \dots, \lambda_{d_x}(\mathbf{u}))^\top$, $\mathbf{q}(\mathbf{g}(\mathbf{x})) := (q_1(g_1(\mathbf{x})), \dots, q_{d_x}(g_{d_x}(\mathbf{x})))^\top$, and note that the Jacobian $|\det \mathbf{J}_{\mathbf{g}}(\mathbf{x})|$ is cancelled out.

On the other hand, by the universal approximation assumption (A4), we obtain

$$\log p(\mathbf{x}|\mathbf{u}) - \log p(\mathbf{x}|\mathbf{u}_0) = (\mathbf{w}(\mathbf{u}) - \mathbf{w}(\mathbf{u}_0))^\top \mathbf{h}(\mathbf{x}) - e(\mathbf{u}) + e(\mathbf{u}_0). \quad (21)$$

Then, equating (20) with (21) provides

$$\bar{\boldsymbol{\lambda}}(\mathbf{u})^\top \mathbf{q}(\mathbf{g}(\mathbf{x})) + \epsilon(\mathbf{u}) \frac{\delta(\mathbf{g}(\mathbf{x})|\mathbf{u})}{p^*(\mathbf{g}(\mathbf{x})|\mathbf{u})} - \epsilon(\mathbf{u}_0) \frac{\delta(\mathbf{g}(\mathbf{x})|\mathbf{u}_0)}{p^*(\mathbf{g}(\mathbf{x})|\mathbf{u}_0)} + O(\epsilon(\mathbf{u})^2) + O(\epsilon(\mathbf{u}_0)^2) = \bar{\mathbf{w}}(\mathbf{u})^\top \mathbf{h}(\mathbf{x}) + \bar{\beta}(\mathbf{u}), \quad (22)$$

where $\bar{\mathbf{w}}(\mathbf{u}) := \mathbf{w}(\mathbf{u}) - \mathbf{w}(\mathbf{u}_0)$, $\bar{\boldsymbol{\lambda}}(\mathbf{u}) := \boldsymbol{\lambda}(\mathbf{u}) - \boldsymbol{\lambda}(\mathbf{u}_0)$, and $\bar{\beta}(\mathbf{u}) := e(\mathbf{u}) - e(\mathbf{u}_0) + \log Z(\boldsymbol{\lambda}(\mathbf{u})) - \log Z(\boldsymbol{\lambda}(\mathbf{u}_0))$.

Next, we multiply $\bar{\boldsymbol{\lambda}}(\mathbf{u})$ to the both sides of (22) and evaluate it at m points, $\mathbf{u}_1, \dots, \mathbf{u}_m$. Finally, taking the summation for $\mathbf{u}_1, \dots, \mathbf{u}_m$ yields

$$\begin{aligned} &\underbrace{\left(\sum_{i=1}^m \bar{\boldsymbol{\lambda}}(\mathbf{u}_i) \bar{\boldsymbol{\lambda}}(\mathbf{u}_i)^\top \right)}_{\bar{\boldsymbol{\Lambda}}} \mathbf{q}(\mathbf{s}) + \sum_{i=1}^m \left(\epsilon(\mathbf{u}_i) \frac{\delta(\mathbf{g}(\mathbf{x})|\mathbf{u}_i)}{p^*(\mathbf{g}(\mathbf{x})|\mathbf{u}_i)} - \epsilon(\mathbf{u}_0) \frac{\delta(\mathbf{g}(\mathbf{x})|\mathbf{u}_0)}{p^*(\mathbf{g}(\mathbf{x})|\mathbf{u}_0)} \right) \bar{\boldsymbol{\lambda}}(\mathbf{u}_i) \\ &\quad + \sum_{i=1}^m \{ O(\epsilon(\mathbf{u}_i)^2) + \epsilon(\mathbf{u}_0)^2 \} \bar{\boldsymbol{\lambda}}(\mathbf{u}_i) = \left(\sum_{i=1}^m \bar{\mathbf{w}}(\mathbf{u}_i) \bar{\boldsymbol{\lambda}}(\mathbf{u}_i)^\top \right) \mathbf{h}(\mathbf{x}) + \sum_{i=1}^m \bar{\beta}(\mathbf{u}_i) \bar{\boldsymbol{\lambda}}(\mathbf{u}_i). \end{aligned}$$

Applying the inverse of $\bar{\boldsymbol{\Lambda}}$ to both sides completes the proof. \square

B Influence of outliers in general non-exponential case

As in Hyvärinen et al. [2019], we assume that the general conditional independence (4) holds, and that both the mixing function \mathbf{f} in the data generative model (1) and a nonlinear feature $\mathbf{h}(\mathbf{x}) = (h_1(\mathbf{x}), \dots, h_{d_x}(\mathbf{x}))^\top$ are invertible. Then, by the change of variables from the generative model (1), \mathbf{s} can be regarded as $\mathbf{h} := \mathbf{h}(\mathbf{x})$:

$$\mathbf{s}(\mathbf{h}) := \mathbf{s} = \mathbf{f}^{-1}(\mathbf{x}) = \mathbf{f}^{-1} \circ \mathbf{h}^{-1}(\mathbf{h}(\mathbf{x})),$$

where \circ denotes composition. For the case of no outliers, Hyvärinen et al. [2019] proved that the nonlinear feature $\mathbf{h}(\mathbf{x})$ asymptotically recover the source \mathbf{s} up to an invertible transformation by confirming that the following conditions hold: For all $i, j, k = 1, \dots, d_x$ but $j \neq k$,

$$\frac{\partial}{\partial h_j} s_i(\mathbf{h}) \frac{\partial}{\partial h_k} s_i(\mathbf{h}) = 0, \text{ and } \frac{\partial^2}{\partial h_j \partial h_k} s_i(\mathbf{h}) = 0. \quad (23)$$

Eq.(23) indicates that each s_i is a function of only one distinct element in the nonlinear feature vector \mathbf{h} , and thus \mathbf{s} is identifiable by $\mathbf{h}(\mathbf{x})$ up to an invertible transformation. Conditions (23) for all i, j, k can be compactly expressed as the following matrix form:

$$\mathbf{M}(\mathbf{s}(\mathbf{h})) = \mathbf{O}, \quad (24)$$

where \mathbf{O} is the null matrix, and $\mathbf{M}(\mathbf{s}(\mathbf{h}))$ is a $(d_x^2 - d_x)$ by $2d_x$ matrix with elements $\frac{\partial}{\partial h_j} s_i(\mathbf{h}) \frac{\partial}{\partial h_k} s_i(\mathbf{h})$ and $\frac{\partial^2}{\partial h_j \partial h_k} s_i(\mathbf{h})$ for all $i, j, k = 1, \dots, d_x$ but $j \neq k$ (i for columns, and j, k for rows in $\mathbf{M}(\mathbf{s}(\mathbf{h}))$).

However, in the presence of outliers, (24) does not hold in general. To investigate the influence from outliers, let us define $\widetilde{\mathbf{M}}(\mathbf{s}(\mathbf{h}))$ by a $(d_x^2 - d_x)$ by $(d_x^2 - d_x)$ matrix whose elements are given by

$$-\frac{\partial}{\partial h_j} s_l(\mathbf{h}) \frac{\partial}{\partial h_k} s_m(\mathbf{h}), \text{ for all } j, k, l, m = 1, \dots, d_x \text{ but } j \neq k \text{ and } l \neq m.$$

Unlike $\mathbf{M}(\mathbf{s}(\mathbf{h}))$, $\widetilde{\mathbf{M}}(\mathbf{s}(\mathbf{h}))$ includes the cross terms related to s_l and s_m for $l \neq m$. The following theorem is useful to understand how (24) is modified by outliers:

Theorem 3. Assume that

(B1) Data \mathbf{x} is generated from (1) where \mathbf{f} is invertible.

(B2) Conditional independence (4) holds in $p^*(\mathbf{s}|\mathbf{u})$.

(B3) For all \mathbf{s} and \mathbf{u} , $\frac{\delta(\mathbf{s}|\mathbf{u})}{p^*(\mathbf{s}|\mathbf{u})}$, $\frac{\delta^l(\mathbf{s}|\mathbf{u})}{p^*(\mathbf{s}|\mathbf{u})}$ and $\frac{\delta^{l,m}(\mathbf{s}|\mathbf{u})}{p^*(\mathbf{s}|\mathbf{u})}$ are finite where $\delta^l(\mathbf{s}|\mathbf{u}) := \frac{\partial}{\partial s_l} \delta(\mathbf{s}|\mathbf{u})$ and $\delta^{l,m}(\mathbf{s}|\mathbf{u}) := \frac{\partial^2}{\partial s_l \partial s_m} \delta(\mathbf{s}|\mathbf{u})$.

(B4) The conditional density of \mathbf{x} given \mathbf{u} is universally approximated with an invertible feature extractor $\mathbf{h}(\mathbf{x}) = (h_1(\mathbf{x}), \dots, h_{d_x}(\mathbf{x}))$ as

$$\log \frac{p(\mathbf{x}|\mathbf{u})}{c(\mathbf{x})e(\mathbf{u})} = \sum_{i=1}^{d_x} \psi(h_i(\mathbf{x}), \mathbf{u}), \quad (25)$$

where ψ , c and e are some functions.

Then, under the contaminated density model (5), the following holds at an arbitrary fixed point \mathbf{u}_0 :

$$\mathbf{M}(\mathbf{s})\mathbf{w}(\mathbf{s}, \mathbf{u}, \mathbf{u}_0) = \widetilde{\mathbf{M}}(\mathbf{s}) \begin{pmatrix} \frac{\partial^2 \{\log p(\mathbf{s}|\mathbf{u}) - \log p(\mathbf{s}|\mathbf{u}_0)\}}{\partial s_1 \partial s_2} \\ \vdots \\ \frac{\partial^2 \{\log p(\mathbf{s}|\mathbf{u}) - \log p(\mathbf{s}|\mathbf{u}_0)\}}{\partial s_{d_x} \partial s_{d_x-1}} \end{pmatrix}, \quad (26)$$

where $\mathbf{w}(\mathbf{s}, \mathbf{u}, \mathbf{u}_0)$ is the $2d_x$ -dimensional vector of $\frac{\partial^2 \{\log p(\mathbf{s}|\mathbf{u}) - \log p(\mathbf{s}|\mathbf{u}_0)\}}{\partial s_i^2}$ and $\frac{\partial \{\log p(\mathbf{s}|\mathbf{u}) - \log p(\mathbf{s}|\mathbf{u}_0)\}}{\partial s_i}$ for $i = 1, \dots, d_x$. Moreover, when $\epsilon(\mathbf{u})$ is sufficiently small, $\frac{\partial^2 \log p(\mathbf{s}|\mathbf{u})}{\partial s_l \partial s_m}$ for $l \neq m$ in the right-hand side of (26) equals to

$$\epsilon(\mathbf{u}) \left\{ q^{*l}(s_l|\mathbf{u}) \frac{\delta^m(\mathbf{s}|\mathbf{u})}{p^*(\mathbf{s}|\mathbf{u})} + q^{*m}(s_m|\mathbf{u}) \frac{\delta^l(\mathbf{s}|\mathbf{u})}{p^*(\mathbf{s}|\mathbf{u})} - q^{*l}(s_l|\mathbf{u}) q^{*m}(s_m|\mathbf{u}) \frac{\delta(\mathbf{s}|\mathbf{u})}{p^*(\mathbf{s}|\mathbf{u})} - \frac{\delta^{l,m}(\mathbf{s}|\mathbf{u})}{p^*(\mathbf{s}|\mathbf{u})} \right\} + O(\epsilon(\mathbf{u})^2), \quad (27)$$

where $q^{*l}(s_l|\mathbf{u}) := \frac{\partial}{\partial s_l} q^*(s_l|\mathbf{u})$.

The proof is given in Section B.1. First of all, in the case of no outliers, Theorem 3 essentially recovers Theorem 1 in Hyvärinen et al. [2019]: When $\epsilon(\mathbf{u}) = 0$ for all \mathbf{u} , $\frac{\partial^2 \log p(\mathbf{s}|\mathbf{u})}{\partial s_l \partial s_m} = 0$ for $l \neq m$ and thus $M(\mathbf{s})\mathbf{w}(\mathbf{s}, \mathbf{u}, \mathbf{u}_0) = \mathbf{O}$, which leads to $M(\mathbf{s}) = \mathbf{O}$ (i.e., Eq.(24)) with an additional assumption that there exist $2d_x + 1$ points, $\mathbf{u}_0, \mathbf{u}_1, \dots, \mathbf{u}_{2d_x}$, such that $\mathbf{w}(\mathbf{s}, \mathbf{u}_1, \mathbf{u}_0), \dots, \mathbf{w}(\mathbf{s}, \mathbf{u}_{2d_x}, \mathbf{u}_0)$ are linear independent.⁵

Again, in the case of no outliers, Hyvärinen et al. [2019] asymptotically satisfies the universal approximation assumption (B4) by applying logistic regression to the binary classification problem (3) where the log-odds ratio, $\log \frac{p(\mathbf{x}, \mathbf{u})}{p(\mathbf{x})p(\mathbf{u})}$, is approximated as the right-hand side of (25) using neural networks. Assumption (B4) is a more general expression than the odds ratio, and indicates that in order to perform nonlinear ICA, it is sufficient that the numerator is the conditional density $p(\mathbf{s}|\mathbf{u})$ or joint density $p(\mathbf{s}, \mathbf{u})$ up to the product of nonzero scalar functions of \mathbf{s} and \mathbf{u} .

However, when $\epsilon(\mathbf{u}) \neq 0$, the right-hand side on (26) is nonzero in general, and thus the source \mathbf{s} cannot be recovered. In particular, $\frac{\partial^2 \log p(\mathbf{s}|\mathbf{u})}{\partial s_l \partial s_m}$ in (26) is the distortion factor, which can be expressed from the four ratios related to the outlier density $\delta(\mathbf{s}|\mathbf{u})$: $\frac{\delta^m(\mathbf{s}|\mathbf{u})}{p^*(\mathbf{s}|\mathbf{u})}$, $\frac{\delta^l(\mathbf{s}|\mathbf{u})}{p^*(\mathbf{s}|\mathbf{u})}$, $\frac{\delta(\mathbf{s}|\mathbf{u})}{p^*(\mathbf{s}|\mathbf{u})}$ and $\frac{\delta^{l,m}(\mathbf{s}|\mathbf{u})}{p^*(\mathbf{s}|\mathbf{u})}$. These ratios can be very large when smooth $\delta(\mathbf{s}|\mathbf{u})$ lies on the tails of $p^*(\mathbf{s}|\mathbf{u})$.

B.1 Proof of Theorem 3

Proof. We first obtain the expression of $\log p(\mathbf{x}|\mathbf{u})$ by the change of variables from $\log p(\mathbf{s}|\mathbf{u})$ through the data generative model (1) as

$$\log p(\mathbf{x}|\mathbf{u}) = \log p(\mathbf{g}(\mathbf{x})|\mathbf{u}) + \log |\det \mathbf{J}_{\mathbf{g}}(\mathbf{x})|,$$

where $\mathbf{g} := \mathbf{f}^{-1}$, \det denotes the determinant and $\mathbf{J}_{\mathbf{g}}(\mathbf{x})$ denotes the Jacobian. Then, the universal approximation assumption (B4) gives

$$\sum_{i=1}^{d_x} \psi(h_i(\mathbf{x}), \mathbf{u}) = \log p(\mathbf{g}(\mathbf{x})|\mathbf{u}) + \log |\det \mathbf{J}_{\mathbf{g}}(\mathbf{x})|.$$

To remove the Jacobian term, we compute the differences of the above equation between \mathbf{u} and a fixed point \mathbf{u}_0 as

$$\sum_{i=1}^{d_x} \bar{\psi}(h_i(\mathbf{x}), \mathbf{u}, \mathbf{u}_0) = \log p(\mathbf{g}(\mathbf{x})|\mathbf{u}) - \log p(\mathbf{g}(\mathbf{x})|\mathbf{u}_0).$$

where

$$\bar{\psi}(h_i(\mathbf{x}), \mathbf{u}, \mathbf{u}_0) := \psi(h_i(\mathbf{x}), \mathbf{u}) - \psi(h_i(\mathbf{x}), \mathbf{u}_0).$$

By the further change of variables $\mathbf{h} = \mathbf{h}(\mathbf{x})$,

$$\sum_{i=1}^{d_x} \bar{\psi}(h_i, \mathbf{u}, \mathbf{u}_0) = \log p(\mathbf{s}(\mathbf{h})|\mathbf{u}) - \log p(\mathbf{s}(\mathbf{h})|\mathbf{u}_0) =: \bar{\varphi}(\mathbf{s}(\mathbf{h}), \mathbf{u}, \mathbf{u}_0), \quad (28)$$

⁵This assumption is called *Assumption of Variability* in Hyvärinen et al. [2019], which implies that the conditional density $p^*(\mathbf{s}|\mathbf{u})$ is sufficiently complex and diverse.

where $\mathbf{s}(\mathbf{h}) := \mathbf{g}(\mathbf{h}^{-1}(\mathbf{h}))$. In the following, we simply express $\mathbf{s}(\mathbf{h})$ as \mathbf{s} whenever the dependency to \mathbf{h} does not matter. Next, let us use the following notations:

$$\begin{aligned}\bar{\varphi}^l(\mathbf{s}, \mathbf{u}, \mathbf{u}_0) &:= \frac{\partial}{\partial s_l} \bar{\varphi}(\mathbf{s}, \mathbf{u}, \mathbf{u}_0), & \bar{\varphi}^{l,m}(\mathbf{s}, \mathbf{u}, \mathbf{u}_0) &:= \frac{\partial^2}{\partial s_l \partial s_m} \bar{\varphi}(\mathbf{s}, \mathbf{u}, \mathbf{u}_0) \\ s_l^k &:= \frac{\partial}{\partial h_k} s_l(\mathbf{h}), & s_l^{jk} &:= \frac{\partial^2}{\partial h_j \partial h_k} s_l(\mathbf{h}) \\ p^l(\mathbf{s}|\mathbf{u}) &:= \frac{\partial}{\partial s_l} p(\mathbf{s}|\mathbf{u}), & p^{l,m}(\mathbf{s}|\mathbf{u}) &:= \frac{\partial^2}{\partial s_l \partial s_m} p(\mathbf{s}|\mathbf{u}) \\ p^{*l}(\mathbf{s}|\mathbf{u}) &:= \frac{\partial}{\partial s_l} p^*(\mathbf{s}|\mathbf{u}), & p^{*,m}(\mathbf{s}|\mathbf{u}) &:= \frac{\partial^2}{\partial s_l \partial s_m} p^*(\mathbf{s}|\mathbf{u})\end{aligned}$$

Taking the second-order partial derivative of the left-hand side on (28) with respect to h_j and h_k for $j \neq k$ yields

$$\frac{\partial^2}{\partial h_j \partial h_k} \sum_{i=1}^{d_x} \bar{\psi}(h_i, \mathbf{u}, \mathbf{u}_0) = 0. \quad (29)$$

On the other hand, the second-order partial derivative of the right-hand side on (28) can be expressed as

$$\frac{\partial^2}{\partial h_j \partial h_k} \bar{\varphi}(\mathbf{s}(\mathbf{h}), \mathbf{u}, \mathbf{u}_0) = \sum_{l=1}^d \left[\bar{\varphi}^{l,l}(\mathbf{s}, \mathbf{u}, \mathbf{u}_0) s_l^j s_l^k + \bar{\varphi}^l(\mathbf{s}, \mathbf{u}, \mathbf{u}_0) s_l^{jk} \right] + \sum_{l=1}^{d_x} \sum_{\substack{m=1 \\ m \neq l}}^{d_x} \bar{\varphi}^{l,m}(\mathbf{s}, \mathbf{u}, \mathbf{u}_0) s_l^j s_m^k. \quad (30)$$

Equating (29) with (30) under (28) gives the following equation:

$$\sum_{l=1}^d \left[\bar{\varphi}^{l,l}(\mathbf{s}, \mathbf{u}, \mathbf{u}_0) s_l^j s_l^k + \bar{\varphi}^l(\mathbf{s}, \mathbf{u}, \mathbf{u}_0) s_l^{jk} \right] = - \sum_{l=1}^{d_x} \sum_{\substack{m=1 \\ m \neq l}}^{d_x} \bar{\varphi}^{l,m}(\mathbf{s}, \mathbf{u}, \mathbf{u}_0) s_l^j s_m^k. \quad (31)$$

Regarding $j = 1, \dots, d_x$ and $k = 1, \dots, d_x$, we collect all of $s_l^j s_l^k$, s_l^{jk} and $-s_l^j s_m^k$ for $j \neq k$ and $l \neq m$ as $(d_x^2 - d_x)$ -dimensional vectors, $\mathbf{a}_l(\mathbf{s})$, $\mathbf{b}_l(\mathbf{s})$, and $\mathbf{c}_{l,m}(\mathbf{s})$, respectively. Then, (31) for all j and k (but $j \neq k$) can be expressed as

$$\sum_{l=1}^d \left[\bar{\varphi}^{l,l}(\mathbf{s}, \mathbf{u}, \mathbf{u}_0) \mathbf{a}_l(\mathbf{s}) + \bar{\varphi}^l(\mathbf{s}, \mathbf{u}, \mathbf{u}_0) \mathbf{b}_l(\mathbf{s}) \right] = \sum_{l=1}^{d_x} \sum_{\substack{m=1 \\ m \neq l}}^{d_x} \bar{\varphi}^{l,m}(\mathbf{s}, \mathbf{u}, \mathbf{u}_0) \mathbf{c}_{l,m}(\mathbf{s}).$$

Furthermore, the above equations for all l and m (but $l \neq m$) can be summarized as the following system of linear equations:

$$\mathbf{M}(\mathbf{s}) \mathbf{w}(\mathbf{s}, \mathbf{u}, \mathbf{u}_0) = \widetilde{\mathbf{M}}(\mathbf{s}) \mathbf{r}(\mathbf{s}, \mathbf{u}, \mathbf{u}_0),$$

where $\mathbf{M}(\mathbf{s}) := (\mathbf{a}_1, \dots, \mathbf{a}_d, \mathbf{b}_1, \dots, \mathbf{b}_d)$, $\widetilde{\mathbf{M}}(\mathbf{s}) := (\mathbf{c}_{1,2}, \mathbf{c}_{1,3}, \dots, \mathbf{c}_{d_x, d_x-1})$, and $\mathbf{w}(\mathbf{s}, \mathbf{u}, \mathbf{u}_0)$ is the $2d_x$ -dimensional vector of all $\bar{\varphi}^{l,l}(\mathbf{s}, \mathbf{u}, \mathbf{u}_0)$ and $\bar{\varphi}^l(\mathbf{s}, \mathbf{u}, \mathbf{u}_0)$, and $\mathbf{r}(\mathbf{s}, \mathbf{u}, \mathbf{u}_0)$ is the $(d_x^2 - d_x)$ -dimensional vector of all $\bar{\varphi}^{l,m}(\mathbf{s}, \mathbf{u}, \mathbf{u}_0)$ for $l \neq m$.

Finally, we prove that $\frac{\partial^2}{\partial s_l \partial s_m} \log p(\mathbf{s}|\mathbf{u})$ for $l \neq m$ equals to (27). We first compute

$$\begin{aligned}
\frac{\partial^2}{\partial s_l \partial s_m} \log p(\mathbf{s}|\mathbf{u}) &= \frac{p^{l,m}(\mathbf{s}|\mathbf{u})p(\mathbf{s}|\mathbf{u}) - p^l(\mathbf{s}|\mathbf{u})p^m(\mathbf{s}|\mathbf{u})}{p(\mathbf{s}|\mathbf{u})^2} \\
&= \frac{p^{l,m}(\mathbf{s}|\mathbf{u})p(\mathbf{s}|\mathbf{u}) - p^l(\mathbf{s}|\mathbf{u})p^m(\mathbf{s}|\mathbf{u})}{p^*(\mathbf{s}|\mathbf{u})^2} (1 + O(\epsilon(\mathbf{u}))) \\
&= (1 - \epsilon(\mathbf{u}))^2 \frac{p^{*l,m}(\mathbf{s}|\mathbf{u})p^*(\mathbf{s}|\mathbf{u}) - p^{*l}(\mathbf{s}|\mathbf{u})p^{*m}(\mathbf{s}|\mathbf{u})}{p^*(\mathbf{s}|\mathbf{u})^2} \\
&\quad + \epsilon(\mathbf{u}) \frac{p^{*l}(\mathbf{s}|\mathbf{u})\delta^m(\mathbf{s}|\mathbf{u}) + p^{*m}(\mathbf{s}|\mathbf{u})\delta^l(\mathbf{s}|\mathbf{u}) - p^{*l,m}(\mathbf{s}|\mathbf{u})\delta(\mathbf{s}|\mathbf{u}) - p^*(\mathbf{s}|\mathbf{u})\delta^{l,m}(\mathbf{s}|\mathbf{u})}{p^*(\mathbf{s}|\mathbf{u})^2} + O(\epsilon(\mathbf{u})^2),
\end{aligned} \tag{32}$$

where we used the contaminated density model (5) on the third line and applied the following relation with a sufficiently small $\epsilon(\mathbf{u})$ on the second line:

$$\frac{1}{p(\mathbf{s}|\mathbf{u})^2} = \frac{1}{\{(1 - \epsilon(\mathbf{u}))p^*(\mathbf{s}|\mathbf{u}) + \epsilon(\mathbf{u})\delta(\mathbf{s}|\mathbf{u})\}^2} = \frac{1}{p^*(\mathbf{s}|\mathbf{u})^2 \left\{1 + \epsilon(\mathbf{u}) \left(\frac{\delta(\mathbf{s}|\mathbf{u})}{p^*(\mathbf{s}|\mathbf{u})} - 1\right)\right\}^2} = \frac{1}{p^*(\mathbf{s}|\mathbf{u})^2} (1 + O(\epsilon(\mathbf{u}))).$$

When $l \neq m$, it can be verified under the conditional independence assumption (B2) that the first term in (32) equals to zero as

$$\frac{p^{*l,m}(\mathbf{s}|\mathbf{u})p^*(\mathbf{s}|\mathbf{u}) - p^{*l}(\mathbf{s}|\mathbf{u})p^{*m}(\mathbf{s}|\mathbf{u})}{p^*(\mathbf{s}|\mathbf{u})^2} = \frac{\partial^2}{\partial s_l \partial s_m} \log p^*(\mathbf{s}|\mathbf{u}) = \frac{\partial}{\partial s_l} q^{*m}(s_m|\mathbf{u}) = 0,$$

Thus, (32) becomes

$$\begin{aligned}
&\frac{\partial^2}{\partial s_l \partial s_m} \log p(\mathbf{s}|\mathbf{u}) \\
&= \epsilon(\mathbf{u}) \left\{ q^{*l}(s_l|\mathbf{u}) \frac{\delta^m(\mathbf{s}|\mathbf{u})}{p^*(\mathbf{s}|\mathbf{u})} + q^{*m}(s_m|\mathbf{u}) \frac{\delta^l(\mathbf{s}|\mathbf{u})}{p^*(\mathbf{s}|\mathbf{u})} - q^{*l}(s_l|\mathbf{u})q^{*m}(s_m|\mathbf{u}) \frac{\delta(\mathbf{s}|\mathbf{u})}{p^*(\mathbf{s}|\mathbf{u})} - \frac{\delta^{l,m}(\mathbf{s}|\mathbf{u})}{p^*(\mathbf{s}|\mathbf{u})} \right\} + O(\epsilon(\mathbf{u})^2),
\end{aligned}$$

where we used

$$\begin{aligned}
\frac{p^{*l}(\mathbf{s}|\mathbf{u})}{p^*(\mathbf{s}|\mathbf{u})} &= \frac{\partial}{\partial s_l} \log p^*(\mathbf{s}|\mathbf{u}) = q^{*l}(s_l|\mathbf{u}) \\
\frac{p^{*l,m}(\mathbf{s}|\mathbf{u})}{p^*(\mathbf{s}|\mathbf{u})} &= \frac{\partial^2}{\partial s_l \partial s_m} \log p^*(\mathbf{s}|\mathbf{u}) + \frac{p^{*l}(\mathbf{s}|\mathbf{u})p^{*m}(\mathbf{s}|\mathbf{u})}{p^*(\mathbf{s}|\mathbf{u})^2} = q^{*l}(s_l|\mathbf{u})q^{*m}(s_m|\mathbf{u}),
\end{aligned}$$

under the conditional independence assumption (B2). Thus, the proof is completed. \square

C Proof of Theorem 2

C.1 Derivation of (13)

With $p(y, \mathbf{x}, \mathbf{u}) = p(\mathbf{x}, \mathbf{u}|y)p(y)$, we have

$$\begin{aligned}
d_\gamma(p(y|\mathbf{x}, \mathbf{u}), r(\mathbf{x}, \mathbf{u}); p(\mathbf{x}, \mathbf{u})) &:= -\frac{1}{\gamma} \log \iint \sum_{y=0}^1 \left\{ \frac{r(\mathbf{x}, \mathbf{u})^{y(\gamma+1)}}{1+r(\mathbf{x}, \mathbf{u})^{\gamma+1}} \right\}^{\frac{\gamma}{\gamma+1}} p(y, \mathbf{x}, \mathbf{u}) d\mathbf{x}d\mathbf{u} \\
&:= -\frac{1}{\gamma} \log \left[\iint \left\{ \frac{r(\mathbf{x}, \mathbf{u})^{\gamma+1}}{1+r(\mathbf{x}, \mathbf{u})^{\gamma+1}} \right\}^{\frac{\gamma}{\gamma+1}} p(\mathbf{x}, \mathbf{u}|y=1)p(y=1) d\mathbf{x}d\mathbf{u} \right. \\
&\quad \left. + \iint \left\{ \frac{1}{1+r(\mathbf{x}, \mathbf{u})^{\gamma+1}} \right\}^{\frac{\gamma}{\gamma+1}} p(\mathbf{x}, \mathbf{u}|y=0)p(y=0) d\mathbf{x}d\mathbf{u} \right] \\
&:= -\frac{1}{\gamma} \log \left[\iint \left\{ \frac{r(\mathbf{x}, \mathbf{u})^{\gamma+1}}{1+r(\mathbf{x}, \mathbf{u})^{\gamma+1}} \right\}^{\frac{\gamma}{\gamma+1}} p(\mathbf{x}, \mathbf{u})p(y=1) d\mathbf{x}d\mathbf{u} \right. \\
&\quad \left. + \iint \left\{ \frac{1}{1+r(\mathbf{x}, \mathbf{u})^{\gamma+1}} \right\}^{\frac{\gamma}{\gamma+1}} p(\mathbf{x})p(\mathbf{u})p(y=0) d\mathbf{x}d\mathbf{u} \right], \quad (33)
\end{aligned}$$

where $p(\mathbf{x}, \mathbf{u}|y=1) = p(\mathbf{x}, \mathbf{u})$, and $p(\mathbf{x}, \mathbf{u}|y=0) = p(\mathbf{x})p(\mathbf{u})$. Under the outlier model, the joint density can be expressed as

$$p(\mathbf{x}, \mathbf{u}) = p(\mathbf{x}|\mathbf{u})p(\mathbf{u}) = (1 - \epsilon(\mathbf{u}))p^*(\mathbf{x}, \mathbf{u}) + \epsilon(\mathbf{u})\delta(\mathbf{x}, \mathbf{u}).$$

Then, the first term inside the logarithm (33) can be written as

$$\begin{aligned}
&\iint \left\{ \frac{r(\mathbf{x}, \mathbf{u})^{\gamma+1}}{1+r(\mathbf{x}, \mathbf{u})^{\gamma+1}} \right\}^{\frac{\gamma}{\gamma+1}} p(\mathbf{x}, \mathbf{u}) d\mathbf{x}d\mathbf{u} \\
&= \iint \left\{ \frac{r(\mathbf{x}, \mathbf{u})^{\gamma+1}}{1+r(\mathbf{x}, \mathbf{u})^{\gamma+1}} \right\}^{\frac{\gamma}{\gamma+1}} (1 - \epsilon(\mathbf{u}))p^*(\mathbf{x}, \mathbf{u}) d\mathbf{x}d\mathbf{u} + \iint \left\{ \frac{r(\mathbf{x}, \mathbf{u})^{\gamma+1}}{1+r(\mathbf{x}, \mathbf{u})^{\gamma+1}} \right\}^{\frac{\gamma}{\gamma+1}} \epsilon(\mathbf{u})\delta(\mathbf{x}, \mathbf{u}) d\mathbf{x}d\mathbf{u} \quad (34)
\end{aligned}$$

Finally, substituting (34) into (33) yields

$$\begin{aligned}
&d_\gamma(p(y|\mathbf{x}, \mathbf{u}), r(\mathbf{x}, \mathbf{u}); p(\mathbf{x}, \mathbf{u})) \\
&:= -\frac{1}{\gamma} \log \left[\frac{1}{2} \iint \left\{ \frac{r(\mathbf{x}, \mathbf{u})^{\gamma+1}}{1+r(\mathbf{x}, \mathbf{u})^{\gamma+1}} \right\}^{\frac{\gamma}{\gamma+1}} (1 - \epsilon(\mathbf{u}))p^*(\mathbf{x}, \mathbf{u}) d\mathbf{x}d\mathbf{u} + \frac{1}{2} \iint \left\{ \frac{1}{1+r(\mathbf{x}, \mathbf{u})^{\gamma+1}} \right\}^{\frac{\gamma}{\gamma+1}} p(\mathbf{x})p(\mathbf{u}) d\mathbf{x}d\mathbf{u} \right. \\
&\quad \left. + \frac{1}{2} \iint \left\{ \frac{r(\mathbf{x}, \mathbf{u})^{\gamma+1}}{1+r(\mathbf{x}, \mathbf{u})^{\gamma+1}} \right\}^{\frac{\gamma}{\gamma+1}} \epsilon(\mathbf{u})\delta(\mathbf{x}, \mathbf{u}) d\mathbf{x}d\mathbf{u} \right] \\
&= J[r(\mathbf{x}, \mathbf{u}); (1 - \epsilon(\mathbf{u}))p^*(\mathbf{x}, \mathbf{u}), p(\mathbf{x})p(\mathbf{u})] + O(\nu),
\end{aligned}$$

where we applied the relation $\log(y+z) = \log(y) + O(z)$ with sufficiently small z .

C.2 Proof of the minimizer (14)

C.2.1 Preliminaries

We use the following results in the main proof, which are derived from the Taylor expansion:

$$\left(\frac{1}{(r + \eta\phi)^{\gamma+1} + 1}\right)^{\frac{\gamma}{\gamma+1}} = \left(\frac{1}{r^{\gamma+1} + 1}\right)^{\frac{\gamma}{\gamma+1}} - \eta \frac{\gamma r^\gamma \phi}{(r^{\gamma+1} + 1)^{\frac{2\gamma+1}{\gamma+1}}} + \frac{\eta^2}{2} \frac{\{\gamma(\gamma+1)r^{2\gamma} - \gamma^2 r^{\gamma-1}\} \phi^2}{(r^{\gamma+1} + 1)^{\frac{3\gamma+1}{\gamma+1}}} + O(\eta^3) \quad (35)$$

$$\left(\frac{(r + \eta\phi)^{\gamma+1}}{(r + \eta\phi)^{\gamma+1} + 1}\right)^{\frac{\gamma}{\gamma+1}} = \left(\frac{r^{\gamma+1}}{r^{\gamma+1} + 1}\right)^{\frac{\gamma}{\gamma+1}} + \eta \frac{\gamma r^{\gamma-1} \phi}{(r^{\gamma+1} + 1)^{\frac{2\gamma+1}{\gamma+1}}} - \frac{\eta^2}{2} \frac{\{\gamma(\gamma+2)r^{2\gamma-1} - \gamma(\gamma-1)r^{\gamma-2}\} \phi^2}{(r^{\gamma+1} + 1)^{\frac{3\gamma+2}{\gamma+1}}} + O(\eta^3). \quad (36)$$

C.2.2 Main proof

Proof. Let us define $\tilde{J}[r] := \exp(-\gamma J[r(\mathbf{x}, \mathbf{u}); (1 - \epsilon(\mathbf{u}))p^*(\mathbf{x}, \mathbf{u}), p(\mathbf{x})p(\mathbf{u})])$, and then we show a maximizer of $\tilde{J}[r]$ alternative to a minimizer of $J[r(\mathbf{x}, \mathbf{u}); (1 - \epsilon(\mathbf{u}))p^*(\mathbf{x}, \mathbf{u}), p(\mathbf{x})p(\mathbf{u})]$. For $\eta > 0$ and a perturbation ϕ , with (35) and (36), we have

$$\begin{aligned} \tilde{J}[r + \eta\phi] &= \tilde{J}[r] + \frac{\eta}{2} \int \int \left[\frac{\gamma r(\mathbf{x}, \mathbf{u})^{\gamma-1} \phi(\mathbf{x}, \mathbf{u}) \{(1 - \epsilon(\mathbf{u}))p^*(\mathbf{x}, \mathbf{u}) - r(\mathbf{x}, \mathbf{u})p(\mathbf{x})p(\mathbf{u})\}}{(r(\mathbf{x}, \mathbf{u})^{\gamma+1} + 1)^{\frac{2\gamma+1}{\gamma+1}}} \right] d\mathbf{x}d\mathbf{u} \\ &+ \frac{\eta^2}{4} \int \int \left[\frac{\{\gamma(\gamma+1)r(\mathbf{x}, \mathbf{u})^{2\gamma} - \gamma^2 r(\mathbf{x}, \mathbf{u})^{\gamma-1}\} p(\mathbf{x})p(\mathbf{u})\phi(\mathbf{x}, \mathbf{u})^2}{(r(\mathbf{x}, \mathbf{u})^{\gamma+1} + 1)^{\frac{3\gamma+2}{\gamma+1}}} \right. \\ &\quad \left. - \frac{\{\gamma(\gamma+2)r(\mathbf{x}, \mathbf{u})^{2\gamma-1} - \gamma(\gamma-1)r(\mathbf{x}, \mathbf{u})^{\gamma-2}\} (1 - \epsilon(\mathbf{u}))p^*(\mathbf{x}, \mathbf{u})\phi(\mathbf{x}, \mathbf{u})^2}{(r(\mathbf{x}, \mathbf{u})^{\gamma+1} + 1)^{\frac{3\gamma+2}{\gamma+1}}} \right] d\mathbf{x}d\mathbf{u} + O(\eta^3). \quad (37) \end{aligned}$$

The optimality condition is satisfied when the term of order η on the right-hand side of (37) equals to zero for arbitrary ϕ . Thus, an optimizer satisfies the following equation:

$$(1 - \epsilon(\mathbf{u}))p^*(\mathbf{x}, \mathbf{u}) - r(\mathbf{x}, \mathbf{u})p(\mathbf{x})p(\mathbf{u}) = 0.$$

Then, we obtain the optimizer as

$$r^*(\mathbf{x}, \mathbf{u}) = \frac{(1 - \epsilon(\mathbf{u}))p^*(\mathbf{x}, \mathbf{u})}{p(\mathbf{x})p(\mathbf{u})} = \frac{(1 - \epsilon(\mathbf{u}))p^*(\mathbf{x}|\mathbf{u})}{p(\mathbf{x})}.$$

To investigate if r^* is a maximizer of $J[r]$, we compute the term of order η^2 on the right-hand side of (37) at $r = r^*$ as

$$- \int \int \left[\frac{\gamma \{r^*(\mathbf{x}, \mathbf{u})^{2\gamma} + r^*(\mathbf{x}, \mathbf{u})^{\gamma-1}\} p(\mathbf{x})p(\mathbf{u})\phi(\mathbf{x}, \mathbf{u})^2}{(r^*(\mathbf{x}, \mathbf{u})^{\gamma+1} + 1)^{\frac{3\gamma+1}{\gamma+1}}} \right] d\mathbf{x}d\mathbf{u},$$

where we used the relation, $(1 - \epsilon(\mathbf{u}))p^*(\mathbf{x}, \mathbf{u}) = r^*(\mathbf{x}, \mathbf{u})p(\mathbf{x})p(\mathbf{u})$. This shows that the term of order η^2 is negative for any choices of ϕ . Thus, r^* is a maximizer, and the proof is completed. \square

D Proof of Proposition 1

Proof. In the neighborhood of $r^*(\mathbf{x}, \mathbf{u}) = \frac{(1-\epsilon(\mathbf{u}))p^*(\mathbf{x}|\mathbf{u})}{p(\mathbf{x})}$, we can obtain

$$\begin{aligned} \nu &= \iint_{\mathcal{S}, \mathcal{U}} \left\{ \frac{r(\mathbf{x}, \mathbf{u})^{\gamma+1}}{1+r(\mathbf{x}, \mathbf{u})^{\gamma+1}} \right\}^{\frac{\gamma}{\gamma+1}} \epsilon(\mathbf{u}) \delta(\mathbf{x}, \mathbf{u}) d\mathbf{x} d\mathbf{u} \\ &\leq \iint_{\mathcal{S}, \mathcal{U}} \left\{ \frac{p^*(\mathbf{x}|\mathbf{u})^{\gamma+1}}{\{(1-\epsilon(\mathbf{u}))p^*(\mathbf{x}|\mathbf{u})\}^{\gamma+1} + p(\mathbf{x})^{\gamma+1}} \right\}^{\frac{\gamma}{\gamma+1}} \delta(\mathbf{x}|\mathbf{u}) d\mathbf{x} (1-\epsilon(\mathbf{u}))^\gamma \epsilon(\mathbf{u}) p(\mathbf{u}) d\mathbf{u} + O\left(\sup_{\mathbf{x}, \mathbf{u}} |r(\mathbf{x}, \mathbf{u}) - r^*(\mathbf{x}, \mathbf{u})|\right). \end{aligned}$$

Next, we perform the change of variables from \mathbf{x} to \mathbf{s} based on the generative model (1) and have

$$\nu \leq \int_{\mathcal{U}} \left[\int_{\mathcal{S}} \left\{ \frac{p^*(\mathbf{s}|\mathbf{u})^{\gamma+1}}{\{(1-\epsilon(\mathbf{u}))p^*(\mathbf{s}|\mathbf{u})\}^{\gamma+1} + p(\mathbf{s})^{\gamma+1}} \right\}^{\frac{\gamma}{\gamma+1}} \delta(\mathbf{s}|\mathbf{u}) d\mathbf{s} \right] g_\gamma(\mathbf{u}) d\mathbf{u} + O\left(\sup_{\mathbf{x}, \mathbf{u}} |r(\mathbf{x}, \mathbf{u}) - r^*(\mathbf{x}, \mathbf{u})|\right),$$

where $g_\gamma(\mathbf{u}) := (1-\epsilon(\mathbf{u}))^\gamma \epsilon(\mathbf{u}) p(\mathbf{u})$. We note that the ratio inside the integral does not depend on the partition function, and thus the change of variables is possible easily.

Under the assumption that $\mathcal{S}_{\mathbf{u}}^{p^*} \cap \mathcal{S}_{\mathbf{u}}^\delta = \emptyset$, we can easily conform that for $\gamma > 0$,

$$\int_{\mathcal{S}} \left\{ \frac{p^*(\mathbf{s}|\mathbf{u})^{\gamma+1}}{\{(1-\epsilon(\mathbf{u}))p^*(\mathbf{s}|\mathbf{u})\}^{\gamma+1} + p(\mathbf{s})^{\gamma+1}} \right\}^{\frac{\gamma}{\gamma+1}} \delta(\mathbf{s}|\mathbf{u}) d\mathbf{s} = 0.$$

The above equation yields

$$\nu \leq O\left(\sup_{\mathbf{x}, \mathbf{u}} |r(\mathbf{x}, \mathbf{u}) - r^*(\mathbf{x}, \mathbf{u})|\right).$$

Thus, the proof is completed. \square

E Avoiding the influence from $\delta(\mathbf{s}|\mathbf{u})/p^*(\mathbf{s}|\mathbf{u})$

Section 3 already indicated that one of the main factors to hamper estimation in nonlinear ICA might be the large density ratio $\delta(\mathbf{s}|\mathbf{u})/p^*(\mathbf{s}|\mathbf{u})$. The following inequality derived in Section E.1 reveals its connection:

$$\nu \leq \frac{1}{C_\gamma} \int \underbrace{\left[\int p^*(\mathbf{s}|\mathbf{u})^{\gamma+1} \frac{\delta(\mathbf{s}|\mathbf{u})}{p^*(\mathbf{s}|\mathbf{u})} d\mathbf{s} \right]}_{(*)} g_\gamma(\mathbf{u}) d\mathbf{u} + O\left(\sup_{\mathbf{x}, \mathbf{u}} |r(\mathbf{x}, \mathbf{u}) - r^*(\mathbf{x}, \mathbf{u})|\right), \quad (38)$$

where $g_\gamma(\mathbf{u}) := (1-\epsilon(\mathbf{u}))^\gamma \epsilon(\mathbf{u}) p(\mathbf{u})$ and $C_\gamma := \inf_{\mathbf{s}, \mathbf{u}} [\{(1-\epsilon(\mathbf{u}))p^*(\mathbf{s}|\mathbf{u})\}^{\gamma+1} + p(\mathbf{s})^{\gamma+1}]^{\gamma/(\gamma+1)}$ is assumed to be nonzero. Integral (*) implies that using a larger γ would reduce the influence of the density ratio $\delta(\mathbf{s}|\mathbf{u})/p^*(\mathbf{s}|\mathbf{u})$ by multiplying it by the density power $p^*(\mathbf{s}|\mathbf{u})^{\gamma+1}$ in the neighborhood of $r^*(\mathbf{x}, \mathbf{u})$. In contrast, in the limit of $\gamma = 0$, the integral (*) is constant, and therefore logistic regression might not be able to avoid a strong influence from $\delta(\mathbf{s}|\mathbf{u})/p^*(\mathbf{s}|\mathbf{u})$.

E.1 Derivation of Inequality (38)

In the neighborhood of $r^*(\mathbf{x}, \mathbf{u}) = \frac{(1-\epsilon(\mathbf{u}))p^*(\mathbf{x}|\mathbf{u})}{p(\mathbf{x})}$, we obtain

$$\begin{aligned} \nu &= \iint \left\{ \frac{r(\mathbf{x}, \mathbf{u})^{\gamma+1}}{1+r(\mathbf{x}, \mathbf{u})^{\gamma+1}} \right\}^{\frac{\gamma}{\gamma+1}} \epsilon(\mathbf{u}) \delta(\mathbf{x}, \mathbf{u}) d\mathbf{x} d\mathbf{u} \\ &\leq \iint \left\{ \frac{\{(1-\epsilon(\mathbf{u}))p^*(\mathbf{x}, \mathbf{u})\}^{\gamma+1}}{\{(1-\epsilon(\mathbf{u}))p^*(\mathbf{x}, \mathbf{u})\}^{\gamma+1} + \{p(\mathbf{x})p(\mathbf{u})\}^{\gamma+1}} \right\}^{\frac{\gamma}{\gamma+1}} \delta(\mathbf{x}) p(\mathbf{u}) d\mathbf{x} d\mathbf{u} + O\left(\sup_{\mathbf{x}, \mathbf{u}} |r(\mathbf{x}, \mathbf{u}) - r^*(\mathbf{x}, \mathbf{u})|\right) \\ &= \iint \left\{ \frac{p^*(\mathbf{x}|\mathbf{u})^{\gamma+1}}{\{(1-\epsilon(\mathbf{u}))p^*(\mathbf{x}|\mathbf{u})\}^{\gamma+1} + p(\mathbf{x})^{\gamma+1}} \right\}^{\frac{\gamma}{\gamma+1}} \delta(\mathbf{x}|\mathbf{u}) d\mathbf{x} (1-\epsilon(\mathbf{u}))^\gamma \epsilon(\mathbf{u}) p(\mathbf{u}) d\mathbf{u} + O\left(\sup_{\mathbf{x}, \mathbf{u}} |r(\mathbf{x}, \mathbf{u}) - r^*(\mathbf{x}, \mathbf{u})|\right). \end{aligned}$$

Next, we perform the change of variables from \mathbf{x} to \mathbf{s} based on the generative model (1) and have

$$\nu \leq \int \left[\int \left\{ \frac{p^*(\mathbf{s}|\mathbf{u})^{\gamma+1}}{\{(1-\epsilon(\mathbf{u}))p^*(\mathbf{s}|\mathbf{u})\}^{\gamma+1} + p(\mathbf{s})^{\gamma+1}} \right\}^{\frac{\gamma}{\gamma+1}} \delta(\mathbf{s}|\mathbf{u}) d\mathbf{s} \right] g_\gamma(\mathbf{u}) d\mathbf{u} + O\left(\sup_{\mathbf{x}, \mathbf{u}} |r(\mathbf{x}, \mathbf{u}) - r^*(\mathbf{x}, \mathbf{u})|\right),$$

where $g_\gamma(\mathbf{u}) := (1-\epsilon(\mathbf{u}))^\gamma \epsilon(\mathbf{u}) p(\mathbf{u})$. Thus,

$$\begin{aligned} \nu &\leq \frac{1}{C_\gamma} \int \left[\int p^*(\mathbf{s}|\mathbf{u})^\gamma \delta(\mathbf{s}|\mathbf{u}) d\mathbf{s} \right] g_\gamma(\mathbf{u}) d\mathbf{u} + O\left(\sup_{\mathbf{x}, \mathbf{u}} |r(\mathbf{x}, \mathbf{u}) - r^*(\mathbf{x}, \mathbf{u})|\right) \\ &= \frac{1}{C_\gamma} \int \left[\int p^*(\mathbf{s}|\mathbf{u})^{\gamma+1} \frac{\delta(\mathbf{s}|\mathbf{u})}{p^*(\mathbf{s}|\mathbf{u})} d\mathbf{s} \right] g_\gamma(\mathbf{u}) d\mathbf{u} + O\left(\sup_{\mathbf{x}, \mathbf{u}} |r(\mathbf{x}, \mathbf{u}) - r^*(\mathbf{x}, \mathbf{u})|\right), \end{aligned}$$

where $C_\gamma := \inf_{\mathbf{s}, \mathbf{u}} |\{(1-\epsilon(\mathbf{u}))p^*(\mathbf{s}|\mathbf{u})\}^{\gamma+1} + p(\mathbf{s})^{\gamma+1}|$.

F Proof of Proposition 2

Proof. We first derive the following lemma, which shows the form of the influence function:

Lemma 1. *The influence function IF($\bar{\mathbf{x}}, \bar{\mathbf{u}}$) of $\hat{\boldsymbol{\theta}}$ under the γ -cross entropy (11) satisfies*

$$\begin{aligned} C_{\hat{\boldsymbol{\theta}}} \text{IF}(\bar{\mathbf{x}}, \bar{\mathbf{u}}) &= \iint \left\{ A_{\hat{\boldsymbol{\theta}}}(\mathbf{x}, \mathbf{u}) \bar{\delta}_{(\bar{\mathbf{x}}, \bar{\mathbf{u}})}(\mathbf{x}, \mathbf{u}) - B_{\hat{\boldsymbol{\theta}}}(\mathbf{x}, \mathbf{u}) (p^*(\mathbf{x}) \bar{\delta}_{\bar{\mathbf{u}}}(\mathbf{u}) + p^*(\mathbf{u}) \bar{\delta}_{\bar{\mathbf{x}}}(\mathbf{x})) + B_{\hat{\boldsymbol{\theta}}}(\mathbf{x}, \mathbf{u}) p^*(\mathbf{x}) p^*(\mathbf{u}) \right\} d\mathbf{x} d\mathbf{u} \\ &= A_{\hat{\boldsymbol{\theta}}}(\bar{\mathbf{x}}, \bar{\mathbf{u}}) - \int B_{\hat{\boldsymbol{\theta}}}(\mathbf{x}, \bar{\mathbf{u}}) p^*(\mathbf{x}) d\mathbf{x} - \int B_{\hat{\boldsymbol{\theta}}}(\bar{\mathbf{x}}, \mathbf{u}) p^*(\mathbf{u}) d\mathbf{u} + \iint B_{\hat{\boldsymbol{\theta}}}(\mathbf{x}, \mathbf{u}) p^*(\mathbf{x}) p^*(\mathbf{u}) d\mathbf{x} d\mathbf{u}, \end{aligned}$$

where

$$\begin{aligned} L_{\boldsymbol{\theta}}(\mathbf{x}, \mathbf{u}) &= \frac{1}{1+r_{\boldsymbol{\theta}}(\mathbf{x}, \mathbf{u})^{\gamma+1}}, \\ S_{\boldsymbol{\theta}}(\mathbf{x}, \mathbf{u}) &= \{L_{\boldsymbol{\theta}}(\mathbf{x}, \mathbf{u})(1-L_{\boldsymbol{\theta}}(\mathbf{x}, \mathbf{u}))\}^{\gamma/(1+\gamma)}, \\ A_{\boldsymbol{\theta}}(\mathbf{x}, \mathbf{u}) &= L_{\boldsymbol{\theta}}(\mathbf{x}, \mathbf{u})^{1/(1+\gamma)} S_{\boldsymbol{\theta}}(\mathbf{x}, \mathbf{u}) \frac{\partial \log r_{\boldsymbol{\theta}}(\mathbf{x}, \mathbf{u})^{\gamma+1}}{\partial \boldsymbol{\theta}}, \\ B_{\boldsymbol{\theta}}(\mathbf{x}, \mathbf{u}) &= (1-L_{\boldsymbol{\theta}}(\mathbf{x}, \mathbf{u}))^{1/(1+\gamma)} S_{\boldsymbol{\theta}}(\mathbf{x}, \mathbf{u}) \frac{\partial \log r_{\boldsymbol{\theta}}(\mathbf{x}, \mathbf{u})^{\gamma+1}}{\partial \boldsymbol{\theta}}, \\ C_{\boldsymbol{\theta}} &= \iint \left\{ \frac{\partial}{\partial \boldsymbol{\theta}} A_{\boldsymbol{\theta}}(\mathbf{x}, \mathbf{u})^\top p^*(\mathbf{x}, \mathbf{u}), -\frac{\partial}{\partial \boldsymbol{\theta}} B_{\boldsymbol{\theta}}(\mathbf{x}, \mathbf{u})^\top p^*(\mathbf{x}) p^*(\mathbf{u}) \right\} d\mathbf{x} d\mathbf{u}. \end{aligned}$$

Let us prove Lemma 1. $\hat{\theta}$ associated with the densities $p^*(\mathbf{x}, \mathbf{u})$ and $p^*(\mathbf{x})p^*(\mathbf{u})$ is a solution of the following estimating equation:

$$\mathbf{0} = \frac{\partial}{\partial \theta} d_\gamma(p^*(y|\mathbf{x}, \mathbf{u}), r_\theta(\mathbf{x}, \mathbf{u}); p^*(\mathbf{x}, \mathbf{u})) \Big|_{\theta=\hat{\theta}} \quad (39)$$

$$\propto \left[\iint \left\{ \left(\frac{r_\theta(\mathbf{x}, \mathbf{u})^{(\gamma+1)}}{1+r_\theta(\mathbf{x}, \mathbf{u})^{(\gamma+1)}} \right)^{-1/(1+\gamma)} \frac{\partial_\theta r_\theta(\mathbf{x}, \mathbf{u})^{(\gamma+1)}}{(1+r_\theta(\mathbf{x}, \mathbf{u})^{(\gamma+1)})^2} p^*(\mathbf{x}, \mathbf{u}) \right. \right. \\ \left. \left. - \left(\frac{1}{1+r_\theta(\mathbf{x}, \mathbf{u})^{(\gamma+1)}} \right)^{-1/(1+\gamma)} \frac{\partial_\theta r_\theta(\mathbf{x}, \mathbf{u})^{(\gamma+1)}}{(1+r_\theta(\mathbf{x}, \mathbf{u})^{(\gamma+1)})^2} p^*(\mathbf{x})p^*(\mathbf{u}) \right\} d\mathbf{x}d\mathbf{u} \right] \Big|_{\theta=\hat{\theta}}, \quad (40)$$

where $\partial_\theta := \frac{\partial}{\partial \theta}$. On the other hand, $\hat{\theta}_\epsilon$ is a solution of the the estimating equation with the contaminated distributions:

$$\mathbf{0} = \frac{\partial}{\partial \theta} d_\gamma(\bar{p}(y|\mathbf{x}, \mathbf{u}), r_\theta(\mathbf{x}, \mathbf{u}); \bar{p}(\mathbf{x}, \mathbf{u})) \Big|_{\theta=\hat{\theta}_\epsilon} \\ \propto \left[\iint \left\{ \left(\frac{r_\theta(\mathbf{x}, \mathbf{u})^{(\gamma+1)}}{1+r_\theta(\mathbf{x}, \mathbf{u})^{(\gamma+1)}} \right)^{-1/(1+\gamma)} \frac{\partial_\theta r_\theta(\mathbf{x}, \mathbf{u})^{(\gamma+1)}}{(1+r_\theta(\mathbf{x}, \mathbf{u})^{(\gamma+1)})^2} \bar{p}(\mathbf{x}, \mathbf{u}) \right. \right. \\ \left. \left. - \left(\frac{1}{1+r_\theta(\mathbf{x}, \mathbf{u})^{(\gamma+1)}} \right)^{-1/(1+\gamma)} \frac{\partial_\theta r_\theta(\mathbf{x}, \mathbf{u})^{(\gamma+1)}}{(1+r_\theta(\mathbf{x}, \mathbf{u})^{(\gamma+1)})^2} \bar{p}(\mathbf{x})\bar{p}(\mathbf{u}) \right\} d\mathbf{x}d\mathbf{u} \right] \Big|_{\theta=\hat{\theta}_\epsilon}. \quad (41)$$

Taylor series of (41) around $\hat{\theta}$ is given by

$$\mathbf{0} = \frac{\partial d_\gamma}{\partial \theta} \Big|_{\theta=\hat{\theta}} + \frac{\partial^2 d_\gamma}{\partial \theta \partial \theta^\top} \Big|_{\theta=\hat{\theta}} (\hat{\theta}_\epsilon - \hat{\theta}) + O(\|\hat{\theta}_\epsilon - \hat{\theta}\|^2). \quad (42)$$

Taking the limit of $\epsilon \rightarrow 0$ proves Lemma 1 using (40).

Since $L_\theta(\mathbf{x}, \mathbf{u})^{1/(1+\gamma)} \leq 1$, we observe that

$$\lim_{|r_\theta(\mathbf{x}, \mathbf{u})| \rightarrow \infty} A_\theta(\mathbf{x}, \mathbf{u}) = \lim_{|r_\theta(\mathbf{x}, \mathbf{u})| \rightarrow \infty} B_\theta(\mathbf{x}, \mathbf{u}) = 0, \quad (43)$$

under Assumption (16). Eq.(43) ensures that the influence function in Lemma 1 is bounded even when $r_{\hat{\theta}}(\bar{\mathbf{x}}, \bar{\mathbf{u}})$, $r_{\hat{\theta}}(\bar{\mathbf{x}}, \mathbf{u})$ or $r_{\hat{\theta}}(\mathbf{x}, \bar{\mathbf{u}})$ diverge through the influence of the outliers $(\bar{\mathbf{x}}, \bar{\mathbf{u}})$, *i.e.*,

$$\sup_{\bar{\mathbf{x}}, \bar{\mathbf{u}}} |\text{IF}(\bar{\mathbf{x}}, \bar{\mathbf{u}})| < \infty. \quad (44)$$

Thus, the proof is completed. \square

G Robust property in multiclass classification

We specifically assume that the following $\tilde{\nu}$ is sufficiently small:

$$\tilde{\nu} := \int \frac{\sum_u r(u, \mathbf{x})^\gamma \delta(\mathbf{x}|u) \epsilon(u) p(u)}{(\sum_{u'} r(u', \mathbf{x})^{\gamma+1})^{\frac{\gamma}{\gamma+1}}} d\mathbf{x}.$$

Then, the outlier model (5) decomposes the γ -cross entropy (18) into

$$\begin{aligned}
& d_\gamma(p(u|\mathbf{x}), r(u, \mathbf{x}); p(\mathbf{x})) \\
&= -\frac{1}{\gamma} \log \int \frac{\sum_u r(u, \mathbf{x})^\gamma p(u|\mathbf{x})}{(\sum_{u'} r(u', \mathbf{x})^{\gamma+1})^{\frac{\gamma}{\gamma+1}}} p(\mathbf{x}) d\mathbf{x} \\
&= -\frac{1}{\gamma} \log \left[\int \frac{\sum_u r(u, \mathbf{x})^\gamma (1 - \epsilon(u)) p^*(\mathbf{x}|u) p(u)}{(\sum_{u'} r(u', \mathbf{x})^{\gamma+1})^{\frac{\gamma}{\gamma+1}}} d\mathbf{x} + \int \frac{\sum_u r(u, \mathbf{x})^\gamma \delta(\mathbf{x}|u) \epsilon(u) p(u)}{(\sum_{u'} r(u', \mathbf{x})^{\gamma+1})^{\frac{\gamma}{\gamma+1}}} d\mathbf{x} \right] \\
&= d_\gamma(r(u, \mathbf{x}), p^*(\mathbf{x}|u); (1 - \epsilon(u))p(u)) + O(\tilde{\nu}), \tag{45}
\end{aligned}$$

where we employed $\log(y + z) = \log(y) + O(z)$ with sufficiently small z and $p(u|\mathbf{x}) = \frac{p(\mathbf{x}|u)p(u)}{p(\mathbf{x})} = \frac{(1 - \epsilon(u))p^*(\mathbf{x}|u)p(u) + \epsilon(u)\delta(\mathbf{x}|u)p(u)}{p(\mathbf{x})}$, and

$$d_\gamma(r(u, \mathbf{x}), p^*(\mathbf{x}|u); (1 - \epsilon(u))p(u)) := -\frac{1}{\gamma} \log \left[\sum_u \left\{ \int \frac{r(u, \mathbf{x})^\gamma p^*(\mathbf{x}|u)}{(\sum_{u'} r(u', \mathbf{x})^{\gamma+1})^{\frac{\gamma}{\gamma+1}}} d\mathbf{x} \right\} (1 - \epsilon(u))p(u) \right].$$

$d_\gamma(r(u, \mathbf{x}), p^*(\mathbf{x}|u); (1 - \epsilon(u))p(u))$ is the γ -cross entropy to $p^*(\mathbf{x}|u)$ under the measure $(1 - \epsilon(u))p(u)$, and thus is minimized at $r(u, \mathbf{x}) = p^*(\mathbf{x}|u)$. The minimizer is desirable in terms of the universal approximation assumptions (A4) and (B4) because it is the (noncontaminated) target density.

Next, we discuss when $\tilde{\nu}$ is sufficiently small. Following Section D, in the neighborhood of $p^*(\mathbf{x}|u)$,

$$\begin{aligned}
\tilde{\nu} &\leq \sum_u \left\{ \int \frac{p^*(\mathbf{x}|u)^\gamma \delta(\mathbf{x}|u)}{(\sum_{u'} p^*(\mathbf{x}|u')^{\gamma+1})^{\frac{\gamma}{\gamma+1}}} d\mathbf{x} \right\} \epsilon(u)p(u) + O(\sup_{u, \mathbf{x}} |r(u, \mathbf{x}) - p^*(\mathbf{x}|u)|) \\
&= \sum_u \left\{ \int \frac{p^*(\mathbf{s}|u)^\gamma \delta(\mathbf{s}|u)}{(\sum_{u'} p^*(\mathbf{s}|u')^{\gamma+1})^{\frac{\gamma}{\gamma+1}}} d\mathbf{s} \right\} \epsilon(u)p(u) + O(\sup_{u, \mathbf{x}} |r(u, \mathbf{x}) - p^*(\mathbf{x}|u)|), \tag{46}
\end{aligned}$$

where we performed the change of variables from \mathbf{x} to \mathbf{s} under the data generate model (1). Under the same support assumptions of $p^*(\mathbf{s}|u)$ and $\delta(\mathbf{s}|u)$ as Section D, we can make the same implication as Proposition 1: ν can be sufficiently small in the neighborhood of $p^*(\mathbf{x}|u)$ when $p^*(\mathbf{s}|u)$ and $\delta(\mathbf{s}|u)$ are clearly separated. This clear separation possibly happens on a situation where $\delta(\mathbf{s}|u)$ lies on the tails of $p^*(\mathbf{s}|u)$ as in common outlier situations. Thus, the γ -cross entropy for multiclass classification would be also robust against outliers.

References

- S. Amari. *Information Geometry and Its Applications*. Springer, 2016.
- A. Basu, I. Harris, N. Hjort, and M. Jones. Robust and efficient estimation by minimising a density power divergence. *Biometrika*, 85(3):549–559, 1998.
- P. Chen, H. Hung, O. Komori, S.-Y. Huang, and S. Eguchi. Robust independent component analysis via minimum γ -divergence estimation. *IEEE Journal of Selected Topics in Signal Processing*, 7(4):614–624, 2013.
- A. Cichocki and S. Amari. Families of alpha-beta-and gamma-divergences: Flexible and robust measures of similarities. *Entropy*, 12(6):1532–1568, 2010.
- P. Comon. Independent component analysis, a new concept? *Signal Processing*, 36(3):287–314, 1994.
- H. Fujisawa and S. Eguchi. Robust parameter estimation with a small bias against heavy contamination. *Journal of Multivariate Analysis*, 99(9):2053–2081, 2008.

- I. Goodfellow, D. Warde-Farley, M. Mirza, A. Courville, and Y. Bengio. Maxout networks. In *Proceedings of the 30th International Conference on Machine Learning (ICML)*, Proceedings of Machine Learning Research, pages 1319–1327. PMLR, 2013.
- I. Goodfellow, J. Pouget-Abadie, M. Mirza, B. Xu, D. Warde-Farley, S. Ozair, A. Courville, and Y. Bengio. Generative adversarial nets. In *Advances in neural information processing systems (NeurIPS)*, pages 2672–2680, 2014.
- A. Gretton, O. Bousquet, A. Smola, and B. Schölkopf. Measuring statistical dependence with Hilbert-Schmidt norms. In *International conference on algorithmic learning theory*, pages 63–77. Springer, 2005.
- M. Gutmann and A. Hyvärinen. Noise-contrastive estimation of unnormalized statistical models, with applications to natural image statistics. *Journal of Machine Learning Research*, 13:307–361, 2012.
- F. R. Hampel, E. M. Ronchetti, P. J. Rousseeuw, and W. A. Stahel. *Robust statistics: the approach based on influence functions*. John Wiley & Sons, 2011.
- S. Harmeling, A. Ziehe, M. Kawanabe, and K.-R. Müller. Kernel-based nonlinear blind source separation. *Neural Computation*, 15(5):1089–1124, 2003.
- H. Hung, Z.-Y. Jou, and S.-Y. Huang. Robust mislabel logistic regression without modeling mislabel probabilities. *Biometrics*, 74(1):145–154, 2018.
- A. Hyvärinen. Fast and robust fixed-point algorithms for independent component analysis. *IEEE Transactions on Neural Networks*, 10(3):626–634, 1999.
- A. Hyvärinen and H. Morioka. Unsupervised feature extraction by time-contrastive learning and nonlinear ICA. In *Advances in Neural Information Processing Systems (NeurIPS)*, pages 3765–3773, 2016.
- A. Hyvärinen and H. Morioka. Nonlinear ICA of temporally dependent stationary sources. In *Proceedings of the 20th International Conference on Artificial Intelligence and Statistics (AISTATS)*, volume 54, pages 460–469. PMLR, 2017.
- A. Hyvärinen and E. Oja. Independent component analysis: algorithms and applications. *Neural Networks*, 13(4–5): 411–430, 2000.
- A. Hyvärinen and P. Pajunen. Nonlinear independent component analysis: Existence and uniqueness results. *Neural Networks*, 12(3):429–439, 1999.
- A. Hyvärinen, H. Sasaki, and R. E. Turner. Nonlinear ICA using auxiliary variables and generalized contrastive learning. In *Proceedings of the 22th International Conference on Artificial Intelligence and Statistics (AISTATS)*, volume 89, pages 859–868, 2019.
- T. Kanamori and H. Fujisawa. Robust estimation under heavy contamination using unnormalized models. *Biometrika*, 102(3):559–572, 2015.
- T. Kawashima and H. Fujisawa. On difference between two types of γ -divergence for regression. *arXiv:1805.06144*, 2018.
- D. P. Kingma and J. Ba. Adam: A method for stochastic optimization. In *Proceedings of the 3rd International Conference on Learning Representations (ICLR)*, pages 1–15, 2015.
- G. Larsson, M. Maire, and G. Shakhnarovich. Colorization as a proxy task for visual understanding. In *Proceedings of the IEEE Conference on Computer Vision and Pattern Recognition (CVPR)*, pages 6874–6883, 2017.
- F. Locatello, S. Bauer, M. Lucic, G. Raetsch, S. Gelly, B. Schölkopf, and O. Bachem. Challenging common assumptions in the unsupervised learning of disentangled representations. In *Proceedings of the 36th International Conference on Machine Learning (ICML)*, volume 97 of *Proceedings of Machine Learning Research*, pages 4114–4124. PMLR, 2019.

- R. P. Monti, K. Zhang, and A. Hyvarinen. Causal discovery with general non-linear relationships using non-linear ICA. *35th Conference on Uncertainty in Artificial Intelligence (UAI)*, 2019.
- M. Noroozi and P. Favaro. Unsupervised learning of visual representations by solving jigsaw puzzles. In *European Conference on Computer Vision (ECCV)*, pages 69–84. Springer, 2016.
- A. v. d. Oord, Y. Li, and O. Vinyals. Representation learning with contrastive predictive coding. *arXiv:1807.03748*, 2018.
- J. Pearl. *Causality: models, reasoning and inference*, volume 29. Springer, 2000.
- R. A. Poldrack, J. A. Mumford, and T. E. Nichols. *Handbook of functional MRI data analysis*. Cambridge University Press, 2011.
- R. A. Poldrack, T. O. Laumann, O. Koyejo, B. Gregory, A. Hover, M.-Y. Chen, K. J. Gorgolewski, J. Luci, S. J. Joo, R. L. Boyd, S. Hunicke-Smith, Z. B. Simpson, T. Caven, V. Sochat, J. M. Shine, E. Gordon, A. Z. Snyder, B. Adeyemo, S. E. Petersen, D. C. Glahn, D. Reese Mckay, J. E. Curran, H. H. H. Göring, M. A. Carless, J. Blangero, R. Dougherty, A. Leemans, D. A. Handwerker, L. Frick, E. M. Marcotte, and J. A. Mumford. Long-term neural and physiological phenotyping of a single human. *Nature communications*, 6:8885, 2015.
- S. Shimizu, P. O. Hoyer, A. Hyvärinen, and A. Kerminen. A linear non-Gaussian acyclic model for causal discovery. *Journal of Machine Learning Research*, 7:2003–2030, 2006.
- H. Sprekeler, T. Zito, and L. Wiskott. An extension of slow feature analysis for nonlinear blind source separation. *Journal of machine learning research*, 15:921–947, 2014.
- L. Wasserman. *All of nonparametric statistics*. Springer, 2006.
- L. Wiskott and T. Sejnowski. Slow feature analysis: Unsupervised learning of invariances. *Neural computation*, 14(4): 715–770, 2002.